

Mathematical Models and Methods in Applied Sciences
© World Scientific Publishing Company

**HIGH ORDER FINITE DIFFERENCE WENO SCHEMES WITH
POSITIVITY-PRESERVING LIMITER FOR CORRELATED
RANDOM WALK WITH DENSITY-DEPENDENT TURNING
RATES**

YAN JIANG

*Department of Mathematics, University of Science and Technology of China, Hefei, Anhui
230026, P.R. China.
jiangy@mail.ustc.edu.cn.*

CHI-WANG SHU

*Division of Applied Mathematics, Brown University, Providence, Rhode Island, 02912, USA.
shu@dam.brown.edu.*

Mengping Zhang

*Department of Mathematics, University of Science and Technology of China, Hefei, Anhui
230026, P.R. China.
mpzhang@ustc.edu.cn.*

Received (Day Month Year)

Revised (Day Month Year)

Communicated by (xxxxxxxxxx)

In this paper, we discuss high order finite difference weighted essentially non-oscillatory (WENO) schemes, coupled with total variation diminishing (TVD) Runge-Kutta (RK) temporal integration, for solving the semilinear hyperbolic system of a correlated random walk model describing movement of animals and cells in biology. Since the solutions to this system are non-negative, we discuss a positivity-preserving limiter without compromising accuracy. Analysis is performed to justify the maintenance of third order spatial / temporal accuracy when the limiters are applied to a third order finite difference scheme and third order TVD-RK time discretization for solving this model. Numerical results are also provided to demonstrate these methods up to fifth order accuracy.

Keywords: weighted essentially non-oscillatory scheme; high order accuracy; positivity-preserving; correlated random walk.

AMS Subject Classification: 65M06, 65M12, 65M15

2 *Y. Jiang, C.-W. Shu, and M. Zhang*

1. Introduction

In this paper, we consider the random walk model in biology. The system is given as

$$\begin{cases} u_t + \gamma u_x = -\lambda_1 u + \lambda_2 v, & (x, t) \in \mathbb{R} \times [0, T] \\ v_t - \gamma v_x = \lambda_1 u - \lambda_2 v, & (x, t) \in \mathbb{R} \times [0, T] \\ u(x, 0) = u_0(x), \quad v(x, 0) = v_0(x), & x \in \mathbb{R} \end{cases} \quad (1.1)$$

This model describes two kinds of particles moving in opposite directions on a line. $u(x, t)$ and $v(x, t)$ are the densities of left-moving and right-moving individuals. The particles move in a constant speed γ and change their directions with rates λ_1 and λ_2 , respectively.

This model has been studied as the classical Goldstein-Kac theory for correlated random walk in Refs. 4, 7 when the turning rates are constants, $\lambda_1 = \lambda_2 = \frac{\mu}{2}$. Since biological phenomena are complicated, the assumption of a constant speed and constant turning rates may not always be true. Often, individuals in a group change their directions when interacting with their neighbors locally or globally. These interactions can be direct through the neighbors' density^{11,13,5,3,2}, or indirect through the chemicals produced by their neighbors¹². Here, we will consider alignment, attraction and repulsion between individuals. Numerical results in Refs. 11, 13, 3, 2 demonstrate a variety of patterns by using first order upwind and second order Lax-Wendroff schemes. More recently, in Ref. 10, third-order positivity-preserving explicit Runge-Kutta discontinuous Galerkin (RKDG) methods are designed. Weighted essentially non-oscillation (WENO) scheme is another class of popular schemes for solving hyperbolic equations, which has the advantage of simplicity on uniform or smooth meshes as well as better control on spurious oscillations for discontinuous or sharp gradient solutions. In this paper, we will discuss positivity-preserving high order finite difference weighted essentially non-oscillation (WENO) schemes for the correlated random walk model with explicit Runge-Kutta time discretization.

WENO schemes are usually used to approximate hyperbolic conservation laws and the first derivative convection terms in the convection dominated partial differential equations, which give sharp, non-oscillatory discontinuity transitions and at the same time provide high order accurate resolutions for the smooth part of the solution. The first WENO scheme was introduced in 1994 by Liu, Osher and Chan in their pioneering paper⁹, in which a third order accurate finite volume WENO scheme in one space dimension was constructed. In Ref. 6, a general framework is provided to design arbitrary order accurate finite difference WENO schemes, which are more efficient for multi-dimensional calculations. Very high order WENO schemes are documented in Ref. 1. Details about the development and applications of WENO schemes can be found in Ref. 14.

Since the densities $u(x, t)$ and $v(x, t)$ in (1.1) should be positive, it is desirable to have numerical schemes also satisfy this property. Recently, Zhang *et al.* developed a framework to obtain positivity-preserving finite volume and discontinuous Galerkin schemes which are proven to maintain the original high order accuracy of these

schemes^{19,20,21,23}. The work in Ref. 10 followed this approach to design positivity-preserving discontinuous Galerkin methods for the random walk model. Unfortunately, this framework is not easy to be generalized to finite difference schemes. The work in Ref. 22 uses this framework for designing positivity-preserving finite difference WENO schemes, however accuracy can be maintained only away from vacuum. On the other hand, in Refs. 16, 17, Xiong *et al.* developed a parameter maximum principle preserving (MPP) flux limiter for finite difference WENO schemes with total variation diminishing (TVD) Runge-Kutta (RK) temporal integration, following the ideas in Refs. 18, 8. The MPP properties of high order schemes are realized by limiting the high order flux towards a first order monotone flux, where the flux limiters are obtained by decoupling the linear, explicit maximum principle constraints. Analysis on the one-dimensional scalar conservation law was performed in Ref. 16, in which it is shown that the MPP limiter can maintain third order accuracy when applied to third order finite difference schemes with third order TVD Runge-Kutta method. In this paper, we will follow the idea in Ref. 16 to design and analyze positivity-preserving finite difference WENO schemes on the correlated random walk model, which contains global integral source terms and needs modifications to the algorithm as well as its analysis.

The rest of the paper is organized as follows. In Sec. 2, we will introduce our model. A first order upwind scheme is introduced to prove its positivity-preserving property under a suitable CFL condition. A short review of finite difference WENO schemes will be given in Sec. 3. In Sec. 4 we discuss the positivity-preserving limiter to guarantee positivity of the numerical solution. We provide analysis to verify that, when used to a third order finite difference scheme with third order TVD-RK time discretization, the limiter can keep third order accuracy under a suitable CFL condition, for both the source terms and the numerical fluxes. In Sec. 5 we present numerical results to demonstrate our numerical methods. Concluding remarks are given in Sec. 6. The proof of some of the technical lemmas are given in the Appendix.

2. The correlated random walk model

In this paper, we consider the correlated random walk model in Refs. 2, 10. It is a nonlocal one-dimensional hyperbolic system with a constant speed γ and density-dependent turning rate functions. The turning rate functions λ_1, λ_2 are defined as follows

$$\lambda_1 = a_1 + a_2 f(y_1[u, v, x]) = a_1 + a_2 f(0) + a_2 (f(y_1[u, v, x]) - f(0)) \quad (2.1)$$

$$\lambda_2 = a_1 + a_2 f(y_2[u, v, x]) = a_1 + a_2 f(0) + a_2 (f(y_2[u, v, x]) - f(0)) \quad (2.2)$$

where a_1, a_2 are positive constants, $a_1 + a_2 f(0)$ is the autonomous turning rate, and $a_2 (f(y_1[u, v, x]) - f(0))$ and $a_2 (f(y_2[u, v, x]) - f(0))$ are the bias turning rates. Here, we consider the cases with three social interactions: attraction ($y_{1,a}, y_{2,a}$), repulsion

4 *Y. Jiang, C.-W. Shu, and M. Zhang*

$(y_{1,r}, y_{2,r})$ and alignment $(y_{1,al}, y_{2,al})$.

$$\begin{aligned}
 f(y) &= 0.5 + 0.5 \tanh(y - y_0), \quad p = u + v, \\
 y_{1,r}[u, v, x] &= y_{1,r}[u, v, x] - y_{1,a}[u, v, x] + y_{1,al}[u, v, x], \\
 y_{2,r}[u, v, x] &= y_{2,r}[u, v, x] - y_{2,a}[u, v, x] + y_{2,al}[u, v, x], \\
 y_{1,r}[u, v, x] &= q_r \int_0^\infty K_r(s)(p(x+s) - p(x-s))ds, \\
 y_{2,r}[u, v, x] &= q_r \int_0^\infty K_r(s)(p(x-s) - p(x+s))ds, \\
 y_{1,a}[u, v, x] &= q_a \int_0^\infty K_a(s)(p(x+s) - p(x-s))ds, \\
 y_{2,a}[u, v, x] &= q_a \int_0^\infty K_a(s)(p(x-s) - p(x+s))ds, \\
 y_{1,al}[u, v, x] &= q_{al} \int_0^\infty K_{al}(s)(v(x+s) - u(x-s))ds, \\
 y_{2,al}[u, v, x] &= q_{al} \int_0^\infty K_{al}(s)(u(x-s) - v(x+s))ds, \\
 K_i(s) &= \frac{1}{\sqrt{2\pi m_i^2}} \exp(-(s - s_i)^2 / (2m_i^2)), \quad i = r, a, al, \quad s \in [0, \infty)
 \end{aligned}$$

We will study the system (1.1) on the interval $[0, L]$ with periodic boundary conditions

$$u(0, t) = u(L, t), \quad v(0, t) = v(L, t) \quad (2.3)$$

with the solution u, v extended periodically on \mathbb{R} with period L . We assume $L > 2s_i$ for $i = r, al, al$.

Here the parameters are taken as in Refs. 3, 10, listed in Table 1.

Table 1. List of the parameters in the model.

Parameter	Description	Units	Fixed value
γ	Speed	L/T	No
a_1	Turning rate	$1/T$	No
a_2	Turning rate	$1/T$	No
y_0	Shift of the turning function	1	2
q_a	Magnitude of attraction	L/N	No
q_{al}	Magnitude of alignment	L/N	No
q_r	Magnitude of repulsion	L/N	No
s_a	Attraction range	L	1
s_{al}	Alignment range	L	0.5
s_r	Repulsion range	L	0.25
m_a	Width of attraction kernel	L	1/8
m_{al}	Width of alignment kernel	L	0.5/8
m_r	Width of repulsion kernel	L	0.25/8
L	Domain size	L	10

The following lemma is proved in Ref. 10, which shows not only the positivity-preserving property for the densities u and v of the first order upwind scheme but also the positivity-preserving property of the solution to the system (1.1) itself.

Lemma 2.1. ¹⁰: *If the initial conditions $u_0(x)$, $v_0(x)$ are nonnegative, then the first order upwind scheme*

$$\frac{u_j^{n+1} - u_j^n}{\Delta t} + \gamma \frac{u_j^n - u_{j-1}^n}{\Delta x} = -(\lambda_1)_j^n u_j^n + (\lambda_2)_j^n v_j^n \quad (2.4)$$

$$\frac{v_j^{n+1} - v_j^n}{\Delta t} - \gamma \frac{v_{j+1}^n - v_j^n}{\Delta x} = (\lambda_1)_j^n u_j^n - (\lambda_2)_j^n v_j^n \quad (2.5)$$

can maintain positivity under the time step restriction

$$\Delta t \leq \frac{1}{\gamma/\Delta x + a_1 + a_2} \quad (2.6)$$

where u_j^n and v_j^n are approximations to the solutions $u(x_j, t^n)$ and $v(x_j, t^n)$ at the grid point $x_j = j\Delta x$ and time level $t^n = n\Delta t$. The turning rate functions $(\lambda_1)_j^n = \lambda_1(y_1[u^n, v^n, x_j])$ and $(\lambda_2)_j^n = \lambda_2(y_2[u^n, v^n, x_j])$ can be obtained by the rectangular rule.

3. Review of finite difference WENO schemes

In this section, we briefly review finite difference WENO schemes for solving a one-dimensional hyperbolic conservation law

$$\begin{cases} u_t + f(u)_x = 0, & x \in [a, b] \\ u(x, 0) = u_0 \end{cases} \quad (3.1)$$

with periodic boundary conditions. We denote the grid as

$$a = x_{1/2} < x_{3/2} < \dots < x_{N-1/2} < x_{N+1/2} = b$$

with

$$I_i = [x_{i-1/2}, x_{i+1/2}], \quad x_i = \frac{1}{2}(x_{i-1/2} + x_{i+1/2}), \quad \Delta x = \frac{b-a}{N}.$$

On the uniform mesh, a semi-discrete conservative finite difference scheme has the following form

$$\frac{d}{dt} u_i(t) + \frac{1}{\Delta x} (\hat{H}_{i+1/2} - \hat{H}_{i-1/2}) = 0 \quad (3.2)$$

where $u_i(t)$ is an approximation to the point value $u(x_i, t)$, and the numerical flux $\hat{H}_{i+1/2} = \hat{f}(u_{i-p}, \dots, u_{i+q})$ is consistent with the physical flux $f(u)$ and is Lipschitz continuous with respect to all arguments. To achieve a high order accuracy

$$\frac{1}{\Delta x} (\hat{H}_{i+1/2} - \hat{H}_{i-1/2}) = f(u)_x|_{x_i} + O(\Delta x^k) \quad (3.3)$$

the scheme can use the following Lemma¹⁵:

6 *Y. Jiang, C.-W. Shu, and M. Zhang*

Lemma 3.1. ¹⁵ *If a function $h(x)$ satisfies the following relationship*

$$f(u(x)) = \frac{1}{\Delta x} \int_{x-\frac{\Delta x}{2}}^{x+\frac{\Delta x}{2}} h(\xi) d\xi \quad (3.4)$$

then

$$\frac{1}{\Delta x} \left(h\left(x + \frac{\Delta x}{2}\right) - h\left(x - \frac{\Delta x}{2}\right) \right) = f(u(x))_x. \quad (3.5)$$

Therefore, the numerical flux $\hat{H}_{i+1/2}$ can be taken as $h(x_{i+1/2})$, which can be obtained by using a WENO reconstruction from neighboring cell averages of $h(x)$:

$$\bar{h}_j = \frac{1}{\Delta x} \int_{I_j} h(\xi) d\xi = f(u(x_j, t)),$$

$j = i - p, \dots, i + q$.

For stability, it is important that upwinding is used in the construction of the flux. When $f'(u) \geq 0$, a stencil with one more point from the left will be taken to reconstruct $\hat{H}_{i+1/2}$, i.e. $p = q$; otherwise, a stencil with one more point from the right will be used, $p = q - 2$. When $f'(u)$ changes sign over the domain, a flux splitting can be applied. The simplest smooth splitting is the Lax-Friedrichs splitting.

As an example, we will list the procedure on the fifth order finite difference WENO scheme for (3.1):

- (i) Split $f(u)$ into two fluxes $f^+(u)$ and $f^-(u)$ with the property $\partial f^+(u)/\partial u \geq 0$ and $\partial f^-(u)/\partial u \leq 0$. For example, the Lax-Friedrichs splitting:

$$f^\pm(u) = \frac{1}{2}(f(u) \pm \alpha u)$$

where $\alpha = \max_u |f'(u)|$ over the relevant range of u .

- (ii) Identify $\bar{v}_i = f^+(u_i)$ and use the fifth WENO reconstruction to obtain the cell boundary values $v_{i+1/2}^+$ for all i . The upwind stencil is chosen as $S = \{I_{i-2}, \dots, I_{i+2}\}$, and the three small stencils are $S^{(0)} = \{I_i, I_{i+1}, I_{i+2}\}$, $S^{(1)} = \{I_{i-1}, I_i, I_{i+1}\}$, $S^{(2)} = \{I_{i-2}, I_{i-1}, I_i\}$. On all small stencils and the big stencil we use standard reconstruction, obtaining

$$\begin{aligned} v_{i+1/2}^{(0)} &= \frac{1}{3}\bar{v}_i + \frac{5}{6}\bar{v}_{i+1} - \frac{1}{6}\bar{v}_{i+2} \\ v_{i+1/2}^{(1)} &= -\frac{1}{6}\bar{v}_{i-1} + \frac{5}{6}\bar{v}_i + \frac{1}{3}\bar{v}_{i+1} \\ v_{i+1/2}^{(2)} &= \frac{1}{3}\bar{v}_{i-2} - \frac{7}{6}\bar{v}_{i-1} + \frac{11}{6}\bar{v}_i \\ v_{i+1/2}^{big} &= \frac{1}{30}\bar{v}_{i-2} - \frac{13}{60}\bar{v}_{i-1} + \frac{47}{60}\bar{v}_i + \frac{9}{20}\bar{v}_{i+1} - \frac{1}{20}\bar{v}_{i+2} \end{aligned}$$

and the linear weights

$$d_0 = \frac{3}{10}, \quad d_1 = \frac{3}{5}, \quad d_2 = \frac{1}{10}$$

which lead to

$$v_{i+1/2}^{big} = d_0 v_{i+1/2}^{(0)} + d_1 v_{i+1/2}^{(1)} + d_2 v_{i+1/2}^{(2)}.$$

The nonlinear weights are taken as

$$\omega_r = \frac{\alpha_r}{\sum_{s=0}^2 \alpha_s}, \quad r = 0, 1, 2$$

with

$$\alpha_r = \frac{d_r}{(\beta_r + \epsilon)^2}, \quad r = 0, 1, 2$$

Here, $\epsilon = 10^{-6}$ is introduced to avoid the denominator to become 0. β_r is the “smoothness indicators” of the stencil $S^{(r)}$. For the fifth order WENO reconstruction, we have

$$\begin{aligned} \beta_0 &= \frac{13}{12}(\bar{v}_i - 2\bar{v}_{i+1} + \bar{v}_{i+2})^2 + \frac{1}{4}(3\bar{v}_i - 4\bar{v}_{i+1} + \bar{v}_{i+2})^2 \\ \beta_1 &= \frac{13}{12}(\bar{v}_{i-1} - 2\bar{v}_i + \bar{v}_{i+1})^2 + \frac{1}{4}(\bar{v}_{i-1} - \bar{v}_{i+1})^2 \\ \beta_2 &= \frac{13}{12}(\bar{v}_{i-2} - 2\bar{v}_{i-1} + \bar{v}_i)^2 + \frac{1}{4}(\bar{v}_{i-2} - 4\bar{v}_{i-1} + 3\bar{v}_i)^2 \end{aligned}$$

Finally, the WENO reconstruction is $v_{i+1/2}^+ = \sum_{r=0}^2 \omega_r v_{i+1/2}^{(r)}$.

(iii) Take the positive numerical flux as

$$\hat{f}_{i+1/2}^+ = v_{i+1/2}^+.$$

(iv) Identify $\bar{v}_i = f^-(u_i)$ and use the WENO reconstruction to obtain the cell boundary values $v_{i+1/2}^-$ for all i . The upwind stencil is chosen as $S = \{I_{i-1}, \dots, I_{i+3}\}$ and the three small stencils are $S^{(0)} = \{I_{i+1}, I_{i+2}, I_{i+3}\}$, $S^{(1)} = \{I_i, I_{i+1}, I_{i+2}\}$ and $S^{(2)} = \{I_{i-1}, I_i, I_{i+1}\}$. Following a mirror-symmetric (with respect to $i+1/2$) procedure we can obtain the WENO reconstruction $v_{i+1/2}^-$, then we take the negative numerical flux as $\hat{f}_{i+1/2}^- = v_{i+1/2}^-$.

(v) Form the numerical flux as

$$\hat{f}_{i+1/2} = \hat{f}_{i+1/2}^+ + \hat{f}_{i+1/2}^-.$$

For one-dimensional system of conservation laws,

$$u(x, t) = (u^1(x, t), \dots, u^m(x, t))^T$$

is a vector, and

$$f(u) = (f^1(u^1, \dots, u^m), \dots, f^m(u^1, \dots, u^m))^T$$

is also a vector. We could use the WENO reconstruction procedure on each component of u as in the scalar case. For our system which is diagonal, this is equivalent to the procedure of reconstruction in the local characteristic fields, which can effectively eliminate spurious oscillations when there are discontinuities in the solution.

8 *Y. Jiang, C.-W. Shu, and M. Zhang*

4. Positivity-preserving limiter

Here, we follow the idea of the positivity-preserving (PP) limiters in Refs. 16, 17. We describe the procedure and analysis only for the u -component of the system (1.1). Similar results can be easily obtained for the v -component as well.

We use a third order TVD Runge-Kutta time integration as an example,

$$\begin{aligned} u^{(1)} &= u^n + \Delta t L(u^n) \\ u^{(2)} &= \frac{3}{4}u^n + \frac{1}{4}(u^{(1)} + \Delta t L(u^{(1)})) \\ u^{n+1} &= \frac{1}{3}u^n + \frac{2}{3}(u^{(2)} + \Delta t L(u^{(2)})). \end{aligned} \quad (4.1)$$

Here, $L(u^n) = -\frac{1}{\Delta x}(\hat{H}_{j+1/2}^n - \hat{H}_{j-1/2}^n) + \hat{G}_j^n$, where $\hat{H}_{j+1/2}^n$ is the numerical flux from the WENO reconstruction based on u^n , and \hat{G}_j^n is the approximation of the point value of the source term $-\lambda_1[u^n, v^n, x_j]u_j^n + \lambda_2[u^n, v^n, x_j]v_j^n$. Similarly, let $\hat{H}_{j+1/2}^{(1)}$ and $\hat{H}_{j+1/2}^{(2)}$ be the numerical fluxes which are reconstructed based on $u^{(1)}$ and $u^{(2)}$, and let $\hat{G}_j^{(1)}$ and $\hat{G}_j^{(2)}$ be the approximation of the source term point values $-\lambda_1[u^{(1)}, v^{(1)}, x_j]u_j^{(1)} + \lambda_2[u^{(1)}, v^{(1)}, x_j]v_j^{(1)}$ and $-\lambda_1[u^{(2)}, v^{(2)}, x_j]u_j^{(2)} + \lambda_2[u^{(2)}, v^{(2)}, x_j]v_j^{(2)}$. Then the scheme (4.1) can be rewritten as

$$u_j^{n+1} = u_j^n - \lambda(\hat{H}_{j+1/2}^{rk} - \hat{H}_{j-1/2}^{rk}) + \Delta t \hat{G}_j^{rk} \quad (4.2)$$

where

$$\begin{aligned} \hat{H}_{j+1/2}^{rk} &= \frac{1}{6}\hat{H}_{j+1/2}^n + \frac{1}{6}\hat{H}_{j+1/2}^{(1)} + \frac{2}{3}\hat{H}_{j+1/2}^{(2)} \\ \hat{G}_j^{rk} &= \frac{1}{6}\hat{G}_j^n + \frac{1}{6}\hat{G}_j^{(1)} + \frac{2}{3}\hat{G}_j^{(2)} \end{aligned}$$

and $\lambda = \Delta t / \Delta x$. Based on Eq. (4.2), we propose to replace the numerical flux $\hat{H}_{j+1/2}^{rk}$ and the source term \hat{G}_j^{rk} by $\tilde{H}_{j+1/2}^{rk}$ and \tilde{G}_j^{rk} such that

$$u_j^{n+1} = u_j^n - \lambda(\tilde{H}_{j+1/2}^{rk} - \tilde{H}_{j-1/2}^{rk}) + \Delta t \tilde{G}_j^{rk} \geq 0 \quad (4.3)$$

while attempting to maintain the original high order accuracy.

With the definitions of $\tilde{H}_{j+1/2}^{rk}$ and \tilde{G}_j^{rk} , we have the following results:

Lemma 4.1. *Using Taylor expansion, we can get*

$$\tilde{G}_j^{rk} = g[u^n, v^n, x_j] + \frac{\Delta t}{2}(-\lambda_{1,t}u - \lambda_1u_t + \lambda_{2,t}v + \lambda_2v_t)|_j^n + O(\Delta t^2 + \Delta x^3) \quad (4.4)$$

$$\begin{aligned} \tilde{H}_{j+1/2}^{rk} &= \gamma u_j^n + \Delta x \left\{ \left(\frac{1}{2} - \frac{1}{2}\lambda\gamma \right) \gamma u_x + \frac{1}{2}\lambda\gamma g \right\} |_j^n \\ &\quad + \frac{1}{2}\Delta x^2 \left\{ \gamma \left(\frac{1}{3}\lambda^2\gamma^2 - \frac{1}{2}\lambda\gamma + \frac{1}{6} \right) u_{xx} + \lambda\gamma \left(\frac{1}{2} - \frac{1}{3}\lambda\gamma \right) (-\lambda_{1,x}u - \lambda_1u_x + \lambda_{2,x}v + \lambda_2v_x) \right. \\ &\quad \left. + \frac{1}{3}\lambda^2\gamma(-\lambda_{1,t}u - \lambda_1u_t + \lambda_{2,t}v + \lambda_2v_t) \right\} |_j^n \end{aligned}$$

$$+ O(\Delta x^3 + \Delta t^3) \quad (4.5)$$

where $g[u, v, x] = -\lambda_1[u, v, x]u(x, t) + \lambda_2[u, v, x]v(x, t)$.

The proof of this lemma is given in the Appendix.

4.1. Positivity-preserving limiter for the source term

First, we choose the time step

$$\Delta t = \frac{CFL}{\gamma/\Delta x + a_1 + a_2}$$

with $CFL \leq 1$, such that the first order scheme

$$u_j^{n+1} = u_j^n - \lambda(\gamma u_j^n - \gamma u_{j-1}^n) + \Delta t g_j^n$$

is positivity preserving by Lemma 2.1. We denote $\hat{f}_{j+1/2}$ as the first order upwind numerical flux. Then we modify the source term by

$$\tilde{u}_j^{n+1} = u_j^n - \lambda(\hat{f}_{j+1/2}^n - \hat{f}_{j-1/2}^n) + \Delta t \tilde{G}_j^{rk} \quad (4.6)$$

such that $\tilde{u}_j^{n+1} \geq 0$, where

$$\tilde{G}_j^{rk} = r_j(\hat{G}_j^{rk} - g_j^n) + g_j^n. \quad (4.7)$$

Denote $\tilde{u}_j = u_j^n - \lambda(\hat{f}_{j+1/2}^n - \hat{f}_{j-1/2}^n) + \Delta t \hat{G}_j^{rk}$, r_j can be chosen to be

$$r_j = \begin{cases} \min\left(-\frac{u_j^n - \lambda(\hat{f}_{j+1/2}^n - \hat{f}_{j-1/2}^n) + \Delta t g_j^n}{\Delta t(\hat{G}_j^{rk} - g_j^n)}, 1\right), & \text{if } \tilde{u}_j < 0 \\ 1, & \text{otherwise} \end{cases} \quad (4.8)$$

For this PP-limiter for the source term, we have the following theorem:

Theorem 4.1. *We use a third order finite difference spatial discretization and a third order RK time integration for the system. Assume the global error*

$$e_j^n = |u(x_j, t^n) - u_j^n| = O(\Delta x^3 + \Delta t^3), \forall n, j. \quad (4.9)$$

Using the limiter on the source term (4.7), we can get

$$\Delta t |\tilde{G}_j^{rk} - \hat{G}_j^{rk}| = O(\Delta x^3 + \Delta t^3), \forall j \quad (4.10)$$

with $CFL \leq 1$.

To prove Theorem 4.1, we need the following lemma as a tool, whose proof is given in the Appendix.

Lemma 4.2. *: We consider the characteristic line passing through the point (x^*, t^*)*

$$l : x|_l = \gamma(t - t^*) + x^* \quad (4.11)$$

10 *Y. Jiang, C.-W. Shu, and M. Zhang*

We also define $w_1(t; x^*, t^*) = u(\gamma(t - t^*) + x^*, t)$ and $w_2(t; x^*, t^*) = v(\gamma(t - t^*) + x^*, t)$. Then we have the conclusion

$$\begin{aligned} w_1(t; x^*, t^*) &= u(x^*, t^*) + (t - t^*) \cdot g[u(x, t^*), v(x, t^*), x^*] + \frac{1}{2}(t - t^*)^2 \\ &\quad \{-\lambda_{1,t}u - \lambda_1 u_t + \lambda_{2,t}v + \lambda_2 v_t + \gamma(-\lambda_{1,x}u - \lambda_1 u_x + \lambda_{2,x}v + \lambda_2 v_x)\}|_{(x^*, t^*)} \\ &\quad + O((t - t^*)^3) \end{aligned} \quad (4.12)$$

Proof. (Proof of Theorem 4.1)

If $r_j = 1$, the limiter does not take effect. So we just need to consider the case

$$r_j = -\frac{u_j^n - \lambda(\hat{f}_{j+1/2}^n - \hat{f}_{j-1/2}^n) + \Delta t g_j^n}{\Delta t(\hat{G}_j^{rk} - g_j^n)} < 1.$$

This implies

$$\begin{aligned} u_j^n - \lambda(\hat{f}_{j+1/2}^n - \hat{f}_{j-1/2}^n) + \Delta t \hat{G}_j^{rk} &< 0 \\ \tilde{G}_j^{rk} &= \frac{u_j^n - \lambda(\hat{f}_{j+1/2}^n - \hat{f}_{j-1/2}^n)}{-\Delta t} \\ \Delta t(\hat{G}_j^{rk} - \tilde{G}_j^{rk}) &= u_j^n - \lambda(\hat{f}_{j+1/2}^n - \hat{f}_{j-1/2}^n) + \Delta t \hat{G}_j^{rk}. \end{aligned}$$

Since $u_j^n - \lambda(\hat{f}_{j+1/2}^n - \hat{f}_{j-1/2}^n) + \Delta t \hat{G}_j^{rk} < 0$, to obtain (4.10), it is sufficient to show that

$$|u_j^n - \lambda(\hat{f}_{j+1/2}^n - \hat{f}_{j-1/2}^n) + \Delta t \hat{G}_j^{rk}| = O(\Delta x^3 + \Delta t^3).$$

Lemma 4.1 tells us that

$$\hat{G}_j^{rk} = g_j^n + \frac{\Delta t}{2}(-\lambda_{1,t}u - \lambda_1 u_t + \lambda_{2,t}v + \lambda_2 v_t)|_j^n + O(\Delta t^2)$$

Since the first order upwind numerical flux is $\hat{f}_{j+1/2}^n = \gamma u_j^n$, we have

$$\Delta t(\hat{G}_j^{rk} - \tilde{G}_j^{rk}) = (1 - \lambda\gamma)u_j^n + \lambda\gamma u_{j-1}^n + \Delta t g_j^n + \frac{\Delta t^2}{2}(-\lambda_{1,t}u - \lambda_1 u_t + \lambda_{2,t}v + \lambda_2 v_t)|_j^n + O(\Delta t^3)$$

To simplify the notations, we use u_j to denote u_j^n and $u(x)$ to denote $u(x, t^n)$. From our assumption (4.9), the difference between $u(x_j, t^n)$ and u_j^n is of high order (third order). In our proof below, we use $u(x_j, t^n)$ and u_j^n interchangeably when such high order difference allows.

Denote $x_0 \in I_j$ to be the local minimum point in cell I_j . We can expand $\Delta t(\hat{G}_j^{rk} - \tilde{G}_j^{rk})$ at x_0 . Denote $u_0 = u(x_0)$, and $z = (x_j - x_0)/\Delta x$. Thus

$$\begin{aligned} \Delta t(\hat{G}_j^{rk} - \tilde{G}_j^{rk}) &= u_0 + \Delta x\{(z - \lambda\gamma)u_x + \lambda g\} + \Delta x^2\{\frac{1}{2}(z^2 - 2\lambda\gamma z + \lambda\gamma)u_{xx} \\ &\quad + \lambda z(-\lambda_{1,x}u - \lambda_1 u_x + \lambda_{2,x}v + \lambda_2 v_x) + \frac{1}{2}\lambda^2(-\lambda_{1,t}u - \lambda_1 u_t + \lambda_{2,t}v + \lambda_2 v_t)\} \\ &\quad + O(\Delta x^3 + \Delta t^3) \end{aligned}$$

where all unspecified u_x , g and their derivatives are values at the location x_0 .

We first consider the case $x_0 \in (x_{j-1/2}, x_{j+1/2})$, with $u_x = 0, u_{xx} \geq 0$ and $z \in (-\frac{1}{2}, \frac{1}{2})$. Then

$$\begin{aligned}
 & \Delta t(\hat{G}_j^{rk} - \tilde{G}_j^{rk}) \\
 = & u_0 + \Delta t g + \frac{1}{2} \Delta t^2 \{-\lambda_{1,t} u - \lambda_1 u_t + \lambda_{2,t} v + \lambda_2 v_t + \gamma(-\lambda_{1,x} u - \lambda_1 u_x + \lambda_{2,x} v + \lambda_2 v_x)\} \\
 & + \frac{1}{2} \Delta x^2 (z^2 - 2\lambda\gamma z + \lambda\gamma) u_{xx} + \Delta t \Delta x (z - \frac{1}{2} \lambda\gamma) (-\lambda_{1,x} u - \lambda_1 u_x + \lambda_{2,x} v + \lambda_2 v_x) \\
 & + O(\Delta x^3 + \Delta t^3) \\
 = & u(x_0 + (z - \frac{1}{2} \lambda\gamma) \Delta x) + \Delta t g[u, v, x_0 + (z - \frac{1}{2} \lambda\gamma) \Delta x] \\
 & + \frac{1}{2} \Delta t^2 \{-\lambda_{1,t} u - \lambda_1 u_t + \lambda_{2,t} v + \lambda_2 v_t + \gamma(\lambda_{1,x} u - \lambda_1 u_x + \lambda_{2,x} v + \lambda_2 v_x)\}|_{x_0 + (z - \frac{1}{2}) \lambda\gamma \Delta x} \\
 & + \frac{1}{2} \Delta x^2 (-\lambda\gamma z + \lambda\gamma - \frac{1}{4} \lambda^2 \gamma^2) u_{xx}|_{x_0} \\
 & + O(\Delta x^3 + \Delta t^3)
 \end{aligned}$$

We have

$$0 \leq \lambda\gamma = \frac{\Delta t}{\Delta x} \gamma = \frac{CFL \times \gamma}{\gamma + \Delta x(a_1 + a_2)} \leq 1$$

when $CFL \leq 1$. Since $z \in (-\frac{1}{2}, \frac{1}{2})$, we can get

$$-\lambda\gamma z + \lambda\gamma - \frac{1}{4} \lambda^2 \gamma^2 \geq \frac{1}{2} \lambda\gamma - \frac{1}{4} \lambda^2 \gamma^2 \geq 0$$

i.e. $(-\lambda\gamma z + \lambda\gamma - \frac{1}{4} \lambda^2 \gamma^2) u_{xx} \geq 0$. For the first three terms, they are an approximation of $w_1(t^n + \Delta t; x_0 + (z - \frac{1}{2} \lambda\gamma) \Delta x, t^n) \geq 0$ with third order accuracy $O(\Delta x^3 + \Delta t^3)$. In summary, $\Delta t(\hat{G}_j^{rk} - \tilde{G}_j^{rk})$ is equal to some non-negative term within $O(\Delta x^3 + \Delta t^3)$.

In the case $u(x)$ reaches its local minimum $x_0 = x_{j-1/2}$, we have $u_x \geq 0$ and $z = (x_j - x_0)/\Delta x = 1/2$.

Thus

$$\begin{aligned}
 & \Delta t(\hat{G}_j^{rk} - \tilde{G}_j^{rk}) \\
 = & u_{j-1/2} + \Delta x \{(\frac{1}{2} - \lambda\gamma) u_x + \lambda g\} \\
 & + \Delta x^2 \{ \frac{1}{8} u_{xx} + \frac{1}{2} \lambda (-\lambda_{1,x} u - \lambda_1 u_x + \lambda_{2,x} v + \lambda_2 v_x) + \frac{1}{2} \lambda^2 (-\lambda_{1,t} u - \lambda_1 u_t + \lambda_{2,t} v + \lambda_2 v_t) \} \\
 & + O(\Delta x^3 + \Delta t^3) \\
 = & u(x_{j-1/2} + \frac{1}{2} (1 - \lambda\gamma) \Delta x) + \Delta t g[u, v, x_{j-1/2} + \frac{1}{2} (1 - \lambda\gamma) \Delta x] \\
 & + \frac{1}{2} \Delta t^2 \{-\lambda_{1,t} u - \lambda_1 u_t + \lambda_{2,t} v + \lambda_2 v_t + \gamma(-\lambda_{1,x} u - \lambda_1 u_x + \lambda_{2,x} v + \lambda_2 v_x)\}|_{x_{j-1/2} + \frac{1}{2} (1 - \lambda\gamma) \Delta x} \\
 & + \Delta x (-\frac{1}{2} \lambda\gamma) u_x(x_{j-1/2}) + \frac{1}{8} \Delta x^2 \lambda\gamma (2 - \lambda\gamma) u_{xx}(x_{j-1/2})
 \end{aligned}$$

12 *Y. Jiang, C.-W. Shu, and M. Zhang*

$$+ O(\Delta x^3 + \Delta t^3)$$

Let $s = 1 - \frac{1}{2}\lambda\gamma$, then

$$\Delta t(\hat{G}_j^{rk} - \tilde{G}_j^{rk}) = I + II + O(\Delta x^3 + \Delta t^3)$$

where

$$\begin{aligned} I = & u(x_{j-1/2} + \frac{1}{2}(1 - \lambda\gamma)\Delta x - s\Delta x) \\ & + \Delta t \cdot \left\{ -\lambda_1[u, v, x_{j-1/2} + \frac{1}{2}(1 - \lambda\gamma)\Delta x] \cdot u(x_{j-1/2} + \frac{1}{2}(1 - \lambda\gamma)\Delta x - s\Delta x) \right. \\ & + \lambda_2[u, v, x_{j-1/2} + \frac{1}{2}(1 - \lambda\gamma)\Delta x] \cdot v(x_{j-1/2} + \frac{1}{2}(1 - \lambda\gamma)\Delta x) \left. \right\} \\ & + \frac{1}{2}\Delta t^2 \cdot \left\{ -\lambda_{1,t}[u, v, x_{j-1/2} + \frac{1}{2}(1 - \lambda\gamma)\Delta x] \cdot u(x_{j-1/2} + \frac{1}{2}(1 - \lambda\gamma)\Delta x - s\Delta x) \right. \\ & - \lambda_1[u, v, x_{j-1/2} + \frac{1}{2}(1 - \lambda\gamma)\Delta x] \cdot u_t(x_{j-1/2} + \frac{1}{2}(1 - \lambda\gamma)\Delta x - s\Delta x) \\ & + \lambda_{2,t}[u, v, x_{j-1/2} + \frac{1}{2}(1 - \lambda\gamma)\Delta x] \cdot v(x_{j-1/2} + \frac{1}{2}(1 - \lambda\gamma)\Delta x) \\ & + \lambda_2[u, v, x_{j-1/2} + \frac{1}{2}(1 - \lambda\gamma)\Delta x] \cdot v_t(x_{j-1/2} + \frac{1}{2}(1 - \lambda\gamma)\Delta x) \\ & + \gamma(-\lambda_{1,x}[u, v, x_{j-1/2} + \frac{1}{2}(1 - \lambda\gamma)\Delta x] \cdot u(x_{j-1/2} + \frac{1}{2}(1 - \lambda\gamma)\Delta x - s\Delta x) \\ & - \lambda_1[u, v, x_{j-1/2} + \frac{1}{2}(1 - \lambda\gamma)\Delta x] \cdot u_x(x_{j-1/2} + \frac{1}{2}(1 - \lambda\gamma)\Delta x - s\Delta x) \\ & + \lambda_{2,x}[u, v, x_{j-1/2} + \frac{1}{2}(1 - \lambda\gamma)\Delta x] \cdot v(x_{j-1/2} + \frac{1}{2}(1 - \lambda\gamma)\Delta x) \\ & \left. + \lambda_2[u, v, x_{j-1/2} + \frac{1}{2}(1 - \lambda\gamma)\Delta x] \cdot v_x(x_{j-1/2} + \frac{1}{2}(1 - \lambda\gamma)\Delta x) \right\} \\ II = & \Delta x(1 - \lambda\gamma)u_x(x_{j-1/2}) \\ & + \Delta x\Delta t(1 - \frac{1}{2}\lambda\gamma)(-\lambda_1[u, v, x_{j-1/2} + \frac{1}{2}(1 - \lambda\gamma)\Delta x] \cdot u_x(x_{j-1/2})) \end{aligned}$$

We define

$$\begin{aligned} \tilde{u}(x, t) &= u(x - s\Delta x, t), \quad \tilde{v}(x, t) = v(x, t) \\ \tilde{g} &= -\lambda_1[\tilde{u}(x + s\Delta x, t), \tilde{v}(x, t), x]\tilde{u}(x, t) + \lambda_2[\tilde{u}(x + s\Delta x, t), \tilde{v}(x, t), x]\tilde{v}(x, t) \end{aligned}$$

For the new system

$$\begin{cases} \tilde{u}_t + \gamma\tilde{u}_x = \tilde{g}, & (x, t) \in \mathbb{R} \times [t^n, T] \\ \tilde{v}_t - \gamma\tilde{v}_x = -\tilde{g}, & (x, t) \in \mathbb{R} \times [t^n, T] \\ \tilde{u}(x, t^n) = u(x - s\Delta x, t^n), \tilde{v}(x, t^n) = v(x, t^n) \end{cases}$$

using the similar idea of Lemma 2.1, we can prove that \tilde{u} and \tilde{v} satisfy positive preserving principle. Considering the value along the characteristic line

$$l : x|_l = \gamma(t - t^n) + x_{j-1/2} + \frac{1}{2}(1 - \lambda\gamma)\Delta x$$

then we can see that I approximates $\tilde{u}(\gamma\Delta t + x_{j-1/2} + \frac{1}{2}(1-\lambda\gamma)\Delta x, t^n + \Delta t)$ with $O(\Delta x^3 + \Delta t^3)$.

Since

$$\begin{aligned}
 & 1 - \lambda\gamma + (1 - \frac{1}{2}\lambda\gamma)\Delta t \times (-\lambda_1[u, v, x_{j-1/2} + \frac{1}{2}(1-\lambda\gamma)\Delta x]) \\
 & \geq 1 - \lambda\gamma + (1 - \frac{1}{2}\lambda\gamma) \frac{CFL}{\gamma/\Delta x + a_1 + a_2} (-a_1 - a_2) \\
 & = \frac{1}{\gamma/\Delta x + a_1 + a_2} [(1 - \lambda\gamma) \frac{\gamma}{\Delta x} + (a_1 + a_2)(1 - \lambda\gamma - CFL(1 - \frac{1}{2}\lambda\gamma))] \\
 & \geq \frac{1}{\gamma/\Delta x + a_1 + a_2} [\frac{\gamma}{\Delta x} - \lambda\gamma(\frac{\gamma}{\Delta x} + a_1 + a_2)] \\
 & = \frac{\gamma}{\gamma/\Delta x + a_1 + a_2} [\frac{1}{\Delta x} - \frac{CFL}{\Delta x}] \\
 & \geq 0
 \end{aligned}$$

when $CFL \leq 1$, we have $II \geq 0$.

In summary, when $x_0^{loc} = x_{j-1/2}$, we can also conclude that $\Delta t(\hat{G}_j^{rk} - \tilde{G}_j^{rk})$ is equal to some non-negative term within $O(\Delta x^3 + \Delta t^3)$.

If $x_0 = x_{j+1/2}$, then $u_x(x_{j+1/2}) \leq 0$ and $z = (x_j - x_0)/\Delta x = -1/2$. Thus

$$\begin{aligned}
 & \Delta t(\hat{G}_j^{rk} - \tilde{G}_j^{rk}) \\
 & = u_{j-1/2} + \Delta x((-\frac{1}{2} - \lambda\gamma)u_x + \lambda g) + \Delta x^2\{\frac{1}{2}(\frac{1}{4} + 2\lambda\gamma)u_{xx} \\
 & \quad - \frac{1}{2}\lambda(-\lambda_{1,x}u - \lambda_1u_x + \lambda_{2,x}v + \lambda_2v_x) + \frac{1}{2}\lambda^2(-\lambda_{1,t}u - \lambda_1u_t + \lambda_{2,t}v + \lambda_2v_t)\} \\
 & \quad + O(\Delta x^3 + \Delta t^3) \\
 & = u(x_{j+1/2} - \frac{1}{2}(1 + \lambda\gamma)\Delta x) + \Delta t g[u, v, x_{j+1/2} - \frac{1}{2}(1 + \lambda\gamma)\Delta x] \\
 & \quad + \frac{1}{2}\Delta t^2\{-\lambda_{1,t}u - \lambda_1u_t + \lambda_{2,t}v + \lambda_2v_t + \gamma(-\lambda_{1,x}u - \lambda_1u_x + \lambda_{2,x}v + \lambda_2v_x)\}_{|x_{j+1/2} - \frac{1}{2}(1 + \lambda\gamma)\Delta x} \\
 & \quad + \Delta x(-\frac{1}{2}\lambda\gamma)u_x(x_{j+1/2}) + \Delta x^2\frac{1}{8}\lambda\gamma(6 - \lambda\gamma)u_{xx}(x_{j+1/2}) + O(\Delta x^3 + \Delta t^3)
 \end{aligned}$$

Denote $s = -\frac{1+\lambda\gamma+\sqrt{1+8\lambda\gamma}}{2} \leq 0$, then

$$\Delta t(\hat{G}_j^{rk} - \tilde{G}_j^{rk}) = I + II + O(\Delta x^3 + \Delta t^3)$$

where

$$\begin{aligned}
 I & = u(x_{j+1/2} - \frac{1}{2}(1 + \lambda\gamma)\Delta x - s\Delta x) \\
 & \quad + \Delta t\{-\lambda_1[u, v, x_{j+1/2} - \frac{1}{2}(1 + \lambda\gamma)\Delta x] \cdot u(x_{j+1/2} - \frac{1}{2}(1 + \lambda\gamma)\Delta x - s\Delta x) \\
 & \quad + \lambda_2[u, v, x_{j+1/2} - \frac{1}{2}(1 + \lambda\gamma)\Delta x] \cdot v(x_{j+1/2} - \frac{1}{2}(1 + \lambda\gamma)\Delta x)\}
 \end{aligned}$$

14 *Y. Jiang, C.-W. Shu, and M. Zhang*

$$\begin{aligned}
 & + \frac{1}{2}\Delta t^2 \left\{ -\lambda_{1,t}[u, v, x_{j+1/2} - \frac{1}{2}(1 + \lambda\gamma)\Delta x] \cdot u(x_{j+1/2} - \frac{1}{2}(1 + \lambda\gamma)\Delta x - s\Delta x) \right. \\
 & - \lambda_1[u, v, x_{j+1/2} - \frac{1}{2}(1 + \lambda\gamma)\Delta x] \cdot u_t(x_{j+1/2} - \frac{1}{2}(1 + \lambda\gamma)\Delta x - s\Delta x) \\
 & + \lambda_{2,t}[u, v, x_{j+1/2} - \frac{1}{2}(1 + \lambda\gamma)\Delta x] \cdot v(x_{j+1/2} - \frac{1}{2}(1 + \lambda\gamma)\Delta x) \\
 & + \lambda_2[u, v, x_{j+1/2} - \frac{1}{2}(1 + \lambda\gamma)\Delta x] \cdot v_t(x_{j+1/2} - \frac{1}{2}(1 + \lambda\gamma)\Delta x) \\
 & + \gamma(-\lambda_{1,x}[u, v, x_{j+1/2} - \frac{1}{2}(1 + \lambda\gamma)\Delta x] \cdot u(x_{j+1/2} - \frac{1}{2}(1 + \lambda\gamma)\Delta x - s\Delta x) \\
 & - \lambda_1[u, v, x_{j+1/2} - \frac{1}{2}(1 + \lambda\gamma)\Delta x] \cdot u_x(x_{j+1/2} - \frac{1}{2}(1 + \lambda\gamma)\Delta x - s\Delta x) \\
 & + \lambda_{2,x}[u, v, x_{j+1/2} - \frac{1}{2}(1 + \lambda\gamma)\Delta x] \cdot v(x_{j+1/2} - \frac{1}{2}(1 + \lambda\gamma)\Delta x) \\
 & \left. + \lambda_2[u, v, x_{j+1/2} - \frac{1}{2}(1 + \lambda\gamma)\Delta x] \cdot v_x(x_{j+1/2} - \frac{1}{2}(1 + \lambda\gamma)\Delta x) \right\} \\
 II & = \Delta x \left(-\frac{1}{2}\lambda\gamma + s \right) u_x(x_{j+1/2}) \\
 & + \Delta x \Delta t s \cdot \left(-\lambda_1[u, v, x_{j+1/2} - \frac{1}{2}(1 + \lambda\gamma)\Delta x] \cdot u_x(x_{j+1/2}) \right)
 \end{aligned}$$

Similar to the case of $x_0 = x_{j-1/2}$, we can show that I equals to some non-negative term within $O(\Delta x^3 + \Delta t^3)$. For II , since

$$-\frac{1}{2}\lambda\gamma + s - \lambda_1 s \Delta t \leq -\frac{1}{2}\lambda\gamma + s(1 - (a_1 + a_2)\Delta t)$$

and

$$1 - (a_1 + a_2)\Delta t = \frac{\gamma/\Delta x + (1 - CFL)(a_1 + a_2)}{\gamma/\Delta x + a_1 + a_2} \geq 0$$

if $CFL \leq 1$, we can obtain that

$$-\frac{1}{2}\lambda\gamma + s - \lambda_1 s \Delta t \leq 0$$

Hence, we also can get $II \geq 0$.

For all the cases, we can see that $\Delta t(\hat{G}_j^{rk} - \tilde{G}_j^{rk})$ equals to some non-negative term plus $O(\Delta x^3 + \Delta t^3)$. Since we know $\Delta t(\hat{G}_j^{rk} - \tilde{G}_j^{rk}) \leq 0$, we have

$$|\Delta t(\hat{G}_j^{rk} - \tilde{G}_j^{rk})| = O(\Delta x^3 + \Delta t^3). \quad \square$$

4.2. Positivity-preserving limiter for the numerical flux

We would like to modify the numerical flux

$$\tilde{H}_{j+1/2}^{rk} = \theta_{j+1/2}(\hat{H}_{j+1/2}^{rk} - \hat{f}_{j+1/2}^n) + \hat{f}_{j+1/2}^n \quad (4.13)$$

such that

$$u_j^n - \lambda(\tilde{H}_{j+1/2}^{rk} - \tilde{H}_{j-1/2}^{rk}) + \Delta t \tilde{G}_j^{rk} \geq 0 \quad (4.14)$$

We denote $\Gamma_j = -u_j^n + \lambda(\hat{f}_{j+1/2}^n - \hat{f}_{j-1/2}^n) - \Delta t \tilde{G}_j^{rk}$ and $F_{j+1/2} = \hat{H}_{j+1/2}^{rk} - \hat{f}_{j+1/2}^n$. Thus, inequality (4.14) can be rewritten as

$$\lambda\theta_{j-1/2}\hat{F}_{j-1/2} - \lambda\theta_{j+1/2}\hat{F}_{j+1/2} - \Gamma_j \geq 0 \quad (4.15)$$

with $\Gamma_j \leq 0$. We need to find a pair $(\Lambda_{-1/2, I_j}, \Lambda_{+1/2, I_j})$ such that any pair $(\theta_{j-1/2}, \theta_{j+1/2}) \in [0, \Lambda_{-1/2, I_j}] \times [0, \Lambda_{+1/2, I_j}]$ would satisfy (4.15).

- (i) If $F_{j-1/2} \geq 0$ and $F_{j+1/2} \leq 0$, the pair would be $(\Lambda_{-1/2, I_j}, \Lambda_{+1/2, I_j}) = (1, 1)$;
- (ii) If $F_{j-1/2} \geq 0$ and $F_{j+1/2} > 0$, the pair can be given as $(\Lambda_{-1/2, I_j}, \Lambda_{+1/2, I_j}) = (1, \min(1, \frac{\Gamma_j}{-\lambda F_{j+1/2}}))$;
- (iii) If $F_{j-1/2} < 0$ and $F_{j+1/2} \leq 0$, the pair can be given as $(\Lambda_{-1/2, I_j}, \Lambda_{+1/2, I_j}) = (\min(1, \frac{\Gamma_j}{\lambda F_{j-1/2}}, 1), 1)$;
- (iv) If $F_{j-1/2} < 0$ and $F_{j+1/2} > 0$, when $(\theta_{j-1/2}, \theta_{j+1/2}) = (1, 1)$ satisfies (4.15), the pair can be given as $(\Lambda_{-1/2, I_j}, \Lambda_{+1/2, I_j}) = (1, 1)$. However, in the case that the pair $(\Lambda_{-1/2, I_j}, \Lambda_{+1/2, I_j}) = (1, 1)$ does not satisfy (4.15), intersection is given as the pair $(\Lambda_{-1/2, I_j}, \Lambda_{+1/2, I_j}) = (\frac{\Gamma_j}{\lambda F_{j-1/2} - \lambda F_{j+1/2}}, \frac{\Gamma_j}{\lambda F_{j-1/2} - \lambda F_{j+1/2}})$.

Then the new flux will be defined as

$$\begin{aligned} \tilde{H}_{j+1/2}^{rk} &= \Lambda_{j+1/2}(\hat{H}_{j+1/2}^{rk} - \hat{f}_{j+1/2}^n) + \hat{f}_{j+1/2}^n \\ \Lambda_{j+1/2} &= \min(\Lambda_{+1/2, I_j}, \Lambda_{-1/2, I_{j+1}}) \end{aligned} \quad (4.16)$$

It is easy to check that the new flux defined as (4.16) can satisfy (4.14).

Theorem 4.2. *We use a third order finite difference spatial discretization and a third order RK time discretization for the system. Assume the global error*

$$e_j^n = |u(x_j, t^n) - u_j^n| = O(\Delta x^3 + \Delta t^3), \forall n, j. \quad (4.17)$$

Then using the limiter (4.16), we can get

$$|\hat{H}_{j+1/2}^{rk} - \tilde{H}_{j+1/2}^{rk}| = O(\Delta x^3 + \Delta t^3), \forall j \quad (4.18)$$

with $CFL \leq 1$.

Proof. Let us look at the four cases for the choice of $(\Lambda_{-1/2, I_j}, \Lambda_{+1/2, I_j})$.

For Case 1, the limiter does not take effect.

For Case 4, we only need to consider the situation when $\Lambda_{+1/2, I_j} = \frac{\Gamma_j}{\lambda F_{j-1/2} - \lambda F_{j+1/2}} < 1$, i.e. $\Gamma_j > \lambda F_{j-1/2} - \lambda F_{j+1/2}$.

$$\begin{aligned} \tilde{H}_{j+1/2}^{rk} - \hat{H}_{j+1/2}^{rk} &= \Lambda_{+1/2, I_j}(\hat{H}_{j+1/2}^{rk} - \hat{f}_{j+1/2}^n) + \hat{f}_{j+1/2}^n - \hat{H}_{j+1/2}^{rk} \\ &= (\Lambda_{+1/2, I_j} - 1)(\hat{H}_{j+1/2}^{rk} - \hat{f}_{j+1/2}^n) \\ &= (\frac{\Gamma_j}{\lambda F_{j-1/2} - \lambda F_{j+1/2}} - 1)(\hat{H}_{j+1/2}^{rk} - \hat{f}_{j+1/2}^n) \\ &= \frac{\lambda F_{j-1/2} - \lambda F_{j+1/2} - \Gamma_j}{\lambda F_{j+1/2} - \lambda F_{j-1/2}} F_{j+1/2} \end{aligned}$$

16 *Y. Jiang, C.-W. Shu, and M. Zhang*

It is sufficient to show that $|\frac{\lambda F_{j-1/2} - \lambda F_{j+1/2} - \Gamma_j}{\lambda F_{j+1/2} - \lambda F_{j-1/2}} F_{j+1/2}| = O(\Delta x^3 + \Delta t^3)$. Because $\Gamma_j > \lambda F_{j-1/2} - \lambda F_{j+1/2}$, which means $\lambda F_{j-1/2} - \lambda F_{j+1/2} - \Gamma_j = u_j^n - \lambda(\hat{H}_{j+1/2}^{rk} - \hat{H}_{j-1/2}^{rk}) + \Delta t \tilde{G}_j^{rk} < 0 \leq u(x_j, t^{n+1})$, and $u_j^n - \lambda(\hat{H}_{j+1/2}^{rk} - \hat{H}_{j-1/2}^{rk}) + \Delta t \tilde{G}_j^{rk}$ approximates $u(x_j, t^{n+1})$ within third order accuracy, we can get $|\lambda F_{j-1/2} - \lambda F_{j+1/2} - \Gamma_j| = O(\Delta x^3 + \Delta t^3)$. Since $0 < \frac{F_{j+1/2}}{\lambda F_{j+1/2} - \lambda F_{j-1/2}} \leq \frac{1}{\lambda}$, we have

$$\left| \frac{\lambda F_{j-1/2} - \lambda F_{j+1/2} - \Gamma_j}{\lambda F_{j+1/2} - \lambda F_{j-1/2}} F_{j+1/2} \right| = O(\Delta x^3 + \Delta t^3)$$

For Case 2, (similarly for Case 3), we only need to consider the situation when

$$\Lambda_{+\frac{1}{2}, I_j} = \frac{\Gamma_j}{-\lambda F_{j+1/2}} < 1$$

with

$$\tilde{H}_{j+1/2}^{rk} - \hat{H}_{j+1/2}^{rk} = \frac{u_j^n - \lambda \hat{H}_{j+1/2}^{rk} + \lambda \hat{f}_{j-1/2}^n + \Delta t \tilde{G}_j^{rk}}{\lambda}$$

Since $\frac{\Gamma_j}{-\lambda F_{j+1/2}} < 1$, which equals to $u_j - \lambda \hat{H}_{j+1/2}^{rk} + \lambda \hat{f}_{j-1/2}^n + \Delta t \tilde{G}_j^{rk} < 0$, it is sufficient to verify that

$$|u_j^n - \lambda \hat{H}_{j+1/2}^{rk} + \lambda \hat{f}_{j-1/2}^n + \Delta t \tilde{G}_j^{rk}| = O(\Delta x^3 + \Delta t^3)$$

We have showed that $\Delta t |\tilde{G}_j^{rk} - \hat{G}_j^{rk}| = O(\Delta x^3 + \Delta t^3)$ in Theorem 4.1, so we can alternatively prove that

$$|u_j^n - \lambda \hat{H}_{j+1/2}^{rk} + \lambda \hat{f}_{j-1/2}^n + \Delta t \hat{G}_j^{rk}| = O(\Delta x^3 + \Delta t^3)$$

Using the results in Lemma 4.1 and $\hat{f}_{j-1/2}^n = \gamma u_{j-1}^n$, we can get

$$\begin{aligned} & u_j^n - \lambda \hat{H}_{j+1/2}^{rk} + \lambda \hat{f}_{j-1/2}^n + \Delta t \hat{G}_j^{rk} \\ &= u_0 + \Delta x \left\{ \left(z - \frac{3}{2} \lambda \gamma + \frac{1}{2} \lambda^2 \gamma^2 \right) u_x + \lambda \left(1 - \frac{1}{2} \lambda \gamma \right) g \right\} \\ & \quad + \frac{1}{2} \Delta x^2 \left\{ z^2 + \lambda \gamma (\lambda \gamma - 3) z - \frac{1}{3} \lambda^3 \gamma^3 + \frac{1}{2} \lambda^2 \gamma^2 + \frac{5}{6} \lambda \gamma \right\} u_{xx} \\ & \quad + \Delta t \Delta x \left\{ \left(1 - \frac{1}{2} \lambda \gamma \right) z + \frac{1}{6} \lambda^2 \gamma^2 - \frac{1}{4} \lambda \gamma \right\} (-\lambda_{1,x} u - \lambda_1 u_x + \lambda_{2,x} v + \lambda_2 v_x) \\ & \quad + \frac{1}{2} \Delta t^2 \left(1 - \frac{1}{3} \lambda \gamma \right) (-\lambda_{1,t} u - \lambda_1 u_t + \lambda_{2,t} v + \lambda_2 v_t) \\ & \quad + O(\Delta x^3 + \Delta t^3) \end{aligned}$$

Similar to the procedure in the proof of Theorem 4.1, all unmarked values of u, g and their derivatives are located at (x_0, t^n) , where x_0 is the local minimum point of $u(x, t^n)$ in I_j and $z = (x_j - x_0)/\Delta x$.

If $x_0 \in (x_{j-1/2}, x_{j+1/2})$, then $u_x = 0$, $u_{xx} \geq 0$,

$$u_j^n - \lambda \hat{H}_{j+1/2}^{rk} + \lambda \hat{f}_{j-1/2}^n + \Delta t \hat{G}_j^{rk}$$

$$\begin{aligned}
 &= u_0 + \Delta t(1 - \frac{1}{2}\lambda\gamma)g + \frac{1}{2}\Delta t^2(1 - \frac{1}{3}\lambda\gamma)\{-\lambda_{1,t}u - \lambda_1u_t + \lambda_{2,t}v + \lambda_2v_t \\
 &\quad + \gamma(-\lambda_{1,x}u - \lambda_1u_x + \lambda_{2,x}v + \lambda_2v_x)\} \\
 &\quad + \frac{1}{2}\Delta x^2\{z^2 + \lambda\gamma(\lambda\gamma - 3)z - \frac{1}{3}\lambda^3\gamma^3 + \frac{1}{2}\lambda^2\gamma^2 + \frac{5}{6}\lambda\gamma\} \cdot u_{xx} \\
 &\quad + \Delta t\Delta x\{(1 - \frac{1}{2}\lambda\gamma)z + \frac{1}{3}\lambda^2\gamma^2 - \frac{3}{4}\lambda\gamma\} \cdot (-\lambda_{1,x}u - \lambda_1u_x + \lambda_{2,x}v + \lambda_2v_x) \\
 &\quad + O(\Delta x^3 + \Delta t^3) \\
 &= \frac{(1 - \frac{1}{2}\lambda\gamma)^2}{1 - \frac{1}{3}\lambda\gamma}\{u_0 + \frac{6 - 2\lambda\gamma}{6 - 3\lambda\gamma}\Delta tg + \frac{1}{2}(\frac{6 - 2\lambda\gamma}{6 - 3\lambda\gamma}\Delta t)^2[\lambda_{1,t}u - \lambda_1u_t + \lambda_{2,t}v + \lambda_2v_t \\
 &\quad + \gamma(-\lambda_{1,x}u - \lambda_1u_x + \lambda_{2,x}v + \lambda_2v_x)]\} \\
 &\quad + \frac{\lambda\gamma(-8 + 3\lambda\gamma)}{4(-3 + \lambda\gamma)}u_0 \\
 &\quad + \frac{1}{2}\Delta x^2\{z^2 + \lambda\gamma(\lambda\gamma - 3)z - \frac{1}{3}\lambda^3\gamma^3 + \frac{1}{2}\lambda^2\gamma^2 + \frac{5}{6}\lambda\gamma\} \cdot u_{xx} \\
 &\quad + \Delta t\Delta x\{(1 - \frac{1}{2}\lambda\gamma)z + \frac{1}{3}\lambda^2\gamma^2 - \frac{3}{4}\lambda\gamma\} \cdot (-\lambda_{1,x}u - \lambda_1u_x + \lambda_{2,x}v + \lambda_2v_x) \\
 &\quad + O(\Delta x^3 + \Delta t^3)
 \end{aligned}$$

Denote $s = z + \frac{4\lambda^2\gamma^2 - 9\lambda\gamma}{12 - 6\lambda\gamma}$, then

$$\begin{aligned}
 &u_j^n - \lambda\hat{H}_{j+1/2}^{rk} + \lambda\hat{f}_{j-1/2}^n + \Delta t\hat{G}_j^{rk} \\
 &= \frac{(1 - \frac{1}{2}\lambda\gamma)^2}{1 - \frac{1}{3}\lambda\gamma}\{u(x_0 + s\Delta x) + \frac{6 - 2\lambda\gamma}{6 - 3\lambda\gamma}\Delta tg[u, v, x_0 + s\Delta x] \\
 &\quad + \frac{1}{2}(\frac{6 - 2\lambda\gamma}{6 - 3\lambda\gamma}\Delta t)^2[-\lambda_{1,t}u - \lambda_1u_t + \lambda_{2,t}v + \lambda_2v_t + \gamma(-\lambda_{1,x}u - \lambda_1u_x + \lambda_{2,x}v + \lambda_2v_x)]|_{x_0 + s\Delta x}\} \\
 &\quad + \frac{\lambda\gamma(-8 + 3\lambda\gamma)}{4(-3 + \lambda\gamma)}u_0 \\
 &\quad + \frac{1}{2}\Delta x^2u_{xx}\{z^2 + \lambda^2\gamma^2z - 3\lambda\gamma z - \frac{1}{3}\lambda^3\gamma^3 + \frac{1}{2}\lambda^2\gamma^2 + \frac{5}{6}\lambda\gamma - \frac{(1 - \frac{1}{2}\lambda\gamma)^2}{1 - \frac{1}{3}\lambda\gamma}s^2\} \\
 &\quad + O(\Delta x^3 + \Delta t^3)
 \end{aligned}$$

Using Lemma 4.1, the first term is a third order approximation of $\frac{(1 - \frac{1}{2}\lambda\gamma)^2}{1 - \frac{1}{3}\lambda\gamma}w_1(t^n + \frac{6 - 2\lambda\gamma}{6 - 3\lambda\gamma}\Delta t; x + s\Delta x, t^n)$. We can check that $z^2 + \lambda^2\gamma^2z - 3\lambda\gamma z - \frac{1}{3}\lambda^3\gamma^3 + \frac{1}{2}\lambda^2\gamma^2 + \frac{5}{6}\lambda\gamma - \frac{(1 - \frac{1}{2}\lambda\gamma)^2}{1 - \frac{1}{3}\lambda\gamma}s^2 \geq 0$ when $z \in (-\frac{1}{2}, \frac{1}{2})$ and $\lambda\gamma \in [0, 1]$.

So, $u_j^n - \lambda\hat{H}_{j+1/2}^{rk} + \lambda\hat{f}_{j-1/2}^n + \Delta t\hat{G}_j^{rk}$ approximates some non-negative term $O(\Delta x^3 + \Delta t^3)$.

If $x_0 = x_{j-1/2}$, then $u_x \geq 0$, and $z = \frac{1}{2}$.

$$\begin{aligned}
 &u_j^n - \lambda\hat{H}_{j+1/2}^{rk} + \lambda\hat{f}_{j-1/2}^n + \Delta t\hat{G}_j^{rk} \\
 &= u_{j-1/2} + (1 - \frac{1}{2}\lambda\gamma)\Delta tg + \frac{1}{2}(1 - \frac{1}{3}\lambda\gamma)\Delta t^2\{-\lambda_{1,t}u - \lambda_1u_t + \lambda_{2,t}v + \lambda_2v_t
 \end{aligned}$$

18 *Y. Jiang, C.-W. Shu, and M. Zhang*

$$\begin{aligned}
 & + \gamma(-\lambda_{1,x}u - \lambda_1u_x + \lambda_{2,x}v + \lambda_2v_x)\} \\
 & + \Delta x\left(\frac{1}{2} - \frac{3}{2}\lambda\gamma + \frac{1}{2}\lambda^2\gamma^2\right)u_x \\
 & + \Delta t\Delta x\left(\frac{1}{2} - \lambda\gamma + \frac{1}{3}\lambda^2\gamma^2\right)(-\lambda_{1,x}u - \lambda_1u_x + \lambda_{2,x}v + \lambda_2v_x) \\
 & + \frac{1}{2}\Delta x^2\left(-\frac{1}{3}\lambda^3\gamma^3 + \lambda^2\gamma^2 - \frac{2}{3}\lambda\gamma + \frac{1}{4}\right)u_{xx} \\
 & + O(\Delta x^3 + \Delta t^3)
 \end{aligned}$$

Denote

$$s_1 = \frac{\frac{1}{2} - \lambda\gamma + \frac{1}{3}\lambda^2\gamma^2}{1 - \frac{1}{2}\lambda\gamma}$$

$$s_2 = \sqrt{\frac{\lambda\gamma(-8 + 3\lambda\gamma)}{4(-3 + \lambda\gamma)}\left[-\frac{1}{3}\lambda^3\gamma^3 + \lambda^2\gamma^2 - \frac{2}{3}\lambda\gamma + \frac{1}{4} - \frac{(1 - \frac{1}{2}\lambda\gamma)^2}{1 - \frac{1}{3}\lambda\gamma}\left(s_1 - \frac{1}{6}\right)^2\right]}$$

$$s_3 = \sqrt{\frac{4(-3 + \lambda\gamma)}{\lambda\gamma(-8 + 3\lambda\gamma)}\left[-\frac{1}{3}\lambda^3\gamma^3 + \lambda^2\gamma^2 - \frac{2}{3}\lambda\gamma + \frac{1}{4} - \frac{(1 - \frac{1}{2}\lambda\gamma)^2}{1 - \frac{1}{3}\lambda\gamma}\left(s_1 - \frac{1}{6}\right)^2\right]}$$

Then the equation is

$$u_j^n - \lambda \hat{H}_{j+1/2}^{rk} + \lambda \hat{f}_{j-1/2}^n + \Delta t \hat{G}_j^{rk} = I + II + III + O(\Delta x^3 + \Delta t^3)$$

where

$$\begin{aligned}
 I &= \frac{(1 - \frac{1}{2}\lambda\gamma)^2}{1 - \frac{1}{3}\lambda\gamma} \{u(x_{j-1/2} + s_1\Delta x - \frac{1}{6}\Delta x) \\
 & + \frac{1 - \frac{1}{3}\lambda\gamma}{1 - \frac{1}{2}\lambda\gamma} \Delta t [-\lambda_1[u, v, x_{j-1/2} + s_1\Delta x] \cdot u(x_{j-\frac{1}{2}} + s_1\Delta x - \frac{1}{6}\Delta x) \\
 & + \lambda_2[u, v, x_{j-1/2} + s_1\Delta x] \cdot v(x_{j-\frac{1}{2}} + s_1\Delta x)] \\
 & + \frac{1}{2}\left(\frac{1 - \frac{1}{3}\lambda\gamma}{1 - \frac{1}{2}\lambda\gamma}\right)^2 \Delta t^2 [\\
 & - \lambda_{1,t}[u, v, x_{j-1/2} + s_1\Delta x] \cdot u(x_{j-\frac{1}{2}} + s_1\Delta x - \frac{1}{6}\Delta x) \\
 & - \lambda_1[u, v, x_{j-1/2} + s_1\Delta x] \cdot u_t(x_{j-\frac{1}{2}} + s_1\Delta x - \frac{1}{6}\Delta x) \\
 & + \lambda_{2,t}[u, v, x_{j-1/2} + s_1\Delta x] \cdot v(x_{j-\frac{1}{2}} + s_1\Delta x) \\
 & + \lambda_2[u, v, x_{j-1/2} + s_1\Delta x] \cdot v_t(x_{j-\frac{1}{2}} + s_1\Delta x) \\
 & + \gamma(-\lambda_{1,x}[u, v, x_{j-1/2} + s_1\Delta x] \cdot u(x_{j-\frac{1}{2}} + s_1\Delta x - \frac{1}{6}\Delta x) \\
 & - \lambda_1[u, v, x_{j-1/2} + s_1\Delta x] \cdot u_x(x_{j-\frac{1}{2}} + s_1\Delta x - \frac{1}{6}\Delta x) \\
 & + \lambda_{2,x}[u, v, x_{j-1/2} + s_1\Delta x] \cdot v(x_{j-\frac{1}{2}} + s_1\Delta x)
 \end{aligned}$$

$$\begin{aligned}
 & + \lambda_2[u, v, x_{j-1/2} + s_1\Delta x] \cdot v_x(x_{j-1/2} + s_1\Delta x)]\} \\
 II &= \frac{\lambda\gamma(-8+3\lambda\gamma)}{4(-3+\lambda\gamma)}u(x_{j-1/2} - s_3\Delta x) \\
 & + \Delta x^2(1 - \frac{1}{2}\lambda\gamma)(-\frac{1}{6}\lambda)\lambda_1[u, v, x_{j-1/2} + s_1\Delta x]u_x(x_{j-1/2}) \\
 III &= \Delta x\{\frac{1}{2} - \frac{3}{2}\lambda\gamma + \frac{1}{2}\lambda^2\gamma^2 - \frac{(1 - \frac{1}{2}\lambda\gamma)^2}{1 - \frac{1}{3}\lambda\gamma}(s_1 - \frac{1}{6}) + s_2\}u_x(x_{j-1/2})
 \end{aligned}$$

We can check that

$$\frac{1}{2} - \frac{3}{2}\lambda\gamma + \frac{1}{2}\lambda^2\gamma^2 - \frac{(1 - \frac{1}{2}\lambda\gamma)^2}{1 - \frac{1}{3}\lambda\gamma}(s_1 - \frac{1}{6}\lambda\gamma) + s_2 \geq 0$$

So $III \geq 0$. Considering the value along characteristic lines, we can see that

$$I + O(\Delta x^3 + \Delta t^3) \geq 0$$

Since $\frac{\lambda\gamma(-8+3\lambda\gamma)}{4(-3+\lambda\gamma)} \geq 0$, all we need to consider is $u(x_{j-1/2} - s_3\Delta t) + \Delta x^2\sigma u_x(x_{j-1/2})$, where $\sigma = -\frac{1}{6}\lambda\lambda_1(1 - \frac{1}{2}\lambda\gamma)\frac{4(-3+\lambda\gamma)}{\lambda\gamma(-3+8\lambda\gamma)}$. It is sufficient to prove that $u(x_{j-1/2} - s_3\Delta t) + \Delta x^2\sigma u_x(x_{j-1/2}) \geq 0$ or $u_x(x_{j-1/2}) = O(\Delta x)$. If u is not monotone in $[x_{j-1/2} - s_3\Delta x - \Delta x, x_{j-1/2} - s_3\Delta x]$, then there exists $x^{\#,1} \in [x_{j-1/2} - s_3\Delta x - \Delta x, x_{j-1/2} - s_3\Delta x]$ such that $u_x(x^{\#,1}) = 0$, and $u_x(x_{j-1/2}) = O(\Delta x)$. If u is monotonically decreasing in $[x_{j-1/2} - s_3\Delta x - \Delta x, x_{j-1/2} - s_3\Delta x]$, then there exists $x^{\#,2} \in [x_{j-1/2} - s_3\Delta x, x_{j-1/2}]$ such that $u_x(x^{\#,2}) = 0$, and $u_x(x_{j-1/2}) = O(\Delta x)$. If u is monotonically increasing in $[x_{j-1/2} - s_3\Delta x - \Delta x, x_{j-1/2} - s_3\Delta x]$, assume $u(x_{j-1/2} - s_3\Delta x - \Delta x) - C\Delta x^2 < 0$, where $C = |\sigma|$. There exists $x^{\#,3} \in [x_{j-1/2} - s_3\Delta x - \Delta x, x_{j-1/2} - s_3\Delta x]$ such that

$$u(x_{j-1/2} - s_3\Delta x) = u(x_{j-1/2} - s_3\Delta x - \Delta x) + \Delta x u_x(x^{\#,3}).$$

where $u_x(x^{\#,3}) \geq 0$. Therefore $u_x(x^{\#,3}) \leq C\Delta x u_x(x_{j-1/2})$, i.e. $u_x(x^{\#,3}) = O(\Delta x)$. Thus we can get $u_x(x_{j-1/2}) = O(\Delta x)$, which implies now

$$II + O(\Delta x^3 + \Delta t^3) \geq 0.$$

In the case of $x_0 = x_{j+1/2}$, we can get similar results. The proof is now complete \square

5. Numerical examples

In this section, we will present some numerical results using the schemes discussed above. We will use the third order finite difference WENO scheme and the fifth order finite difference WENO scheme in space, denoted as WENO-3 and WENO-5. Both schemes are combined with the third order TVD Runge-Kutta temporal integration. Without special declaration, the time step is chosen as

$$\Delta t = \frac{CFL}{\gamma/\Delta x + a_1 + a_2} \tag{5.1}$$

20 *Y. Jiang, C.-W. Shu, and M. Zhang*

We take $CFL = 0.6$ in the numerical tests, such that the PP-limiter will not destroy accuracy when $\Delta x \leq 1$. For the infinite integrals, based on the fact that

$$\int_{2s_i}^{\infty} K_i(s) ds \leq 2 \times 10^{-15}, \quad i = r, a, al,$$

we can just compute the integrals on the compact interval $[0, 2s_i]$. Here, the rectangular rule is used, which is the most accurate rule for compactly supported smooth functions. To avoid the effect of rounding error, we change the condition (4.6) and (4.14) into

$$u_j^n - \lambda(\hat{f}_{j+1/2}^n - \hat{f}_{j-1/2}^n) + \Delta t \tilde{G}_j^{rk} \geq \epsilon \quad (5.2)$$

$$u_j^n - \lambda(\tilde{H}_{j+1/2}^{rk} - \tilde{H}_{j-1/2}^{rk}) + \Delta t \tilde{G}_j^{rk} \geq \epsilon \quad (5.3)$$

where $\epsilon = 10^{-16}$.

Example 1. We first test the accuracy with constant coefficients $\lambda_1 = \lambda_2 = 0.5$. The initial condition is

$$u(x, 0) = \begin{cases} (\frac{x(x-4)}{4})^6, & 0 \leq x \leq 4 \\ 0, & 4 < x \leq 10. \end{cases} \quad (5.4)$$

$$v(x, 0) = \begin{cases} 0, & 0 \leq x < 6 \\ (\frac{(x-6)(x-10)}{4})^6, & 6 \leq x \leq 10. \end{cases} \quad (5.5)$$

with 10-periodic boundary condition. Clearly $u(x, 0), v(x, 0) \in C^5(\mathbb{R})$. The final time is $T = 5$. Since the exact solution is not available in closed form, we obtain an accurate reference solution by using the spectral method with 12,800 grid points to serve as the “exact” reference solution.

Table 2. Example 1: Constant coefficients. u -component. WENO-3. Without the PP-limiter.

nx	L_∞ error	order	L_1 error	order	L_2 error	order	min value
40	2.203E-02	–	4.379E-03	–	6.385E-03	–	-1.353E-05
80	6.632E-03	1.732	9.288E-04	2.237	1.615E-03	1.983	-1.297E-05
160	1.595E-03	2.056	1.910E-04	2.281	3.531E-04	2.194	-5.619E-06
320	3.203E-04	2.316	2.963E-05	2.689	6.076E-05	2.539	-3.199E-07
640	3.143E-05	3.349	2.796E-06	3.406	5.793E-06	3.391	-1.603E-08
1280	2.121E-06	3.889	2.484E-07	3.493	4.729E-07	3.615	-7.482E-10

We test the WENO-3 scheme with the time step (5.1) without the PP-limiter and with it. The WENO-5 scheme without the PP-limiter and with it are also tested, with time step

$$\Delta t = \frac{CFL}{(\gamma/\Delta x)^{5/3} + a_1 + a_2} \quad (5.6)$$

Table 3. Example 1: Constant coefficients. u -component. WENO-3. With the PP-limiter.

nx	L_∞ error	order	L_1 error	order	L_2 error	order	min value
40	2.203E-02	–	4.378E-03	–	6.385E-03	–	1.000E-16
80	6.632E-03	1.732	9.281E-04	2.238	1.615E-03	1.983	1.000E-16
160	1.595E-03	2.056	1.909E-04	2.281	3.531E-04	2.194	1.000E-16
320	3.203E-04	2.316	2.963E-05	2.688	6.076E-05	2.539	1.000E-16
640	3.143E-05	3.349	2.796E-06	3.406	5.793E-06	3.391	1.000E-16
1280	2.121E-06	3.889	2.484E-07	3.493	4.729E-07	3.615	1.000E-16

Table 4. Example 1: Constant coefficients. u -component. WENO-5. Without the PP-limiter.

nx	L_∞ error	order	L_1 error	order	L_2 error	order	min value
40	2.006E-03	–	5.064E-04	–	6.640E-04	–	-2.169E-06
80	1.475E-04	3.766	2.776E-05	4.189	3.833E-05	4.115	-2.923E-06
160	7.643E-06	4.270	1.841E-06	3.915	2.559E-06	3.905	-8.671E-08
320	3.899E-07	4.293	1.038E-07	4.148	1.503E-07	4.090	-3.682E-10
640	1.520E-08	4.681	3.940E-09	4.720	5.959E-09	4.656	-1.220E-11
1280	5.035E-10	4.916	1.256E-10	4.972	1.970E-10	4.919	-4.632E-13

Table 5. Example 1: Constant coefficients. u -component. WENO-5. With the PP-limiter.

nx	L_∞ error	order	L_1 error	order	L_2 error	order	min value
40	2.006E-03	–	5.061E-04	–	6.640E-04	–	1.000E-16
80	1.475E-04	3.766	2.777E-05	4.188	3.840E-05	4.112	1.000E-16
160	7.643E-06	4.270	1.840E-06	3.915	2.559E-06	3.907	1.000E-16
320	3.899E-07	4.293	1.038E-07	4.148	1.503E-07	4.090	1.000E-16
640	1.520E-08	4.681	3.940E-09	4.720	5.959E-09	4.656	1.000E-16
1280	5.035E-10	4.916	1.256E-10	4.972	1.970E-10	4.919	1.000E-16

which is designed to match the temporal and spatial orders of accuracy. Errors and orders of accuracy of the u -component are shown in Tables 2-5. The minimum values of numerical solutions at the final time are also listed. It is clear that the PP-limiter can strictly keep the solutions non-negative without loss of accuracy.

Example 2. Next, we test the accuracy for system (1.1) with variable coefficients. We choose the parameters as

$$\begin{aligned} \gamma &= 0.1, & a_1 &= 0.2, & a_2 &= 0.9, \\ q_a &= 1.6, & q_{al} &= 2.0, & q_r &= 0.5. \end{aligned}$$

The same initial conditions are used as in Example 1 (5.4)-(5.5).

In Tables 6-9, we list the order of accuracy and minimum values of the u -component at the final time $T = 5$ of WENO-3 with the time step (5.1) and

Table 6. Example 2: Variable coefficients. u -component. WENO-3. Without the PP-limiter.

nx	L_∞ error	order	L_1 error	order	L_2 error	order	min value
40	7.979E-02	–	1.487E-02	–	2.411E-02	–	-1.900E-05
80	1.436E-02	2.474	2.687E-03	2.468	4.311E-03	2.483	-1.671E-05
160	5.422E-03	1.405	3.487E-04	2.946	8.959E-04	2.266	-1.167E-05
320	1.720E-03	1.656	6.278E-05	2.474	2.236E-04	2.003	-9.804E-07
640	3.278E-04	2.392	7.419E-06	3.081	3.158E-05	2.823	-5.344E-08
1280	2.761E-05	3.569	5.553E-07	3.740	2.205E-06	3.840	-2.671E-09

Table 7. Example 2: Variable coefficients. u -component. WENO-3. With the PP-limiter.

nx	L_∞ error	order	L_1 error	order	L_2 error	order	min value
40	7.979E-02	–	1.486E-02	–	2.411E-02	–	1.000E-16
80	1.436E-02	2.474	2.686E-03	2.468	4.311E-03	2.483	1.000E-16
160	5.422E-03	1.405	3.484E-04	2.946	8.959E-04	2.266	1.000E-16
320	1.720E-03	1.656	6.278E-05	2.473	2.236E-04	2.003	1.000E-16
640	3.278E-04	2.392	7.419E-06	3.081	3.158E-05	2.823	1.000E-16
1280	2.761E-05	3.569	5.553E-07	3.740	2.205E-06	3.840	1.000E-16

Table 8. Example 2: Variable coefficients. u -component. WENO-5. Without the PP-limiter.

nx	L_∞ error	order	L_1 error	order	L_2 error	order	min value
40	7.551E-02	–	1.445E-02	–	2.406E-02	–	-4.538E-06
80	6.932E-03	3.445	1.968E-03	2.876	3.015E-03	2.997	-5.606E-06
160	1.704E-04	5.346	4.622E-05	5.412	7.101E-05	5.408	-6.639E-07
320	4.441E-07	8.584	7.699E-08	9.230	1.185E-07	9.226	-1.255E-09
640	1.572E-08	4.820	2.758E-09	4.803	4.224E-09	4.811	-4.296E-11
1280	5.093E-10	4.948	8.341E-11	5.048	1.301E-10	5.020	-1.792E-12

WENO-5 with the time step (5.6). They show that our schemes can achieve the designed order of accuracy and the PP-limiter can keep positivity without destroying accuracy.

Example 3. In this example, we will test the example of stationary pulses as in ¹⁰. Suppose (u^*, v^*) is the homogeneous steady state with $u^* + v^* = A$, where A is the total population density. When $q_{al} = 0$, we have only one steady state $(u^*, v^* = (A/2, A/2))$. However, when $q_{al} \neq 0$, the system can have one, three or five solutions, and these solutions are obtained by the steady equation from (1.1),

$$-u^*(a_1 + a_2 f(Aq_{al} - 2u^* q_{al} - y_0)) + (A - u^*)(a_1 + a_2 f(-Aq_{al} + 2u^* q_{al} - y_0)) = 0.$$

Table 9. Example 2: Variable coefficients. u -component. WENO-5. With the PP-limiter.

nx	L_∞ error	order	L_1 error	order	L_2 error	order	min value
40	7.551E-02	-	1.445E-02	-	2.406E-02	-	1.000E-16
80	6.932E-03	3.445	1.968E-03	2.876	3.015E-03	2.997	1.000E-16
160	1.704E-04	5.346	4.622E-05	5.412	7.101E-05	5.408	1.000E-16
320	4.441E-07	8.584	7.698E-08	9.230	1.185E-07	9.226	1.000E-16
640	1.572E-08	4.820	2.758E-09	4.803	4.224E-09	4.811	1.000E-16
1280	5.093E-10	4.948	8.341E-11	5.047	1.301E-10	5.020	1.000E-16

We choose the parameters as

$$\begin{aligned} \gamma &= 0.1, & a_1 &= 0.2, & a_2 &= 0.9, \\ q_a &= 2, & q_{al} &= 0, & q_r &= 2.4, \end{aligned}$$

also we choose $A = 2$, which means that the steady state is $(u^*, v^*) = (1, 1)$. The initial conditions are taken as a small perturbation on this steady state

$$\begin{cases} u(x, 0) = 1 + 0.01 \sin(0.2\pi x) \\ v(x, 0) = 1 + 0.005 \cos(0.2\pi x) \end{cases} \quad (5.7)$$

The solution evolves into stationary pulses.

In Figure 1, we plot the numerical solutions of the total density $p = u + v$ from $t = 1500$ to $t = 2000$, using the first order upwind scheme, the third order WENO-3 scheme and the fifth order WENO-5 scheme with $nx = 500$ grid points. We also plot the solution obtained with the first order upwind scheme using 6000 grid points as a converged reference solution. The numerical solutions are stationary for all the schemes. All schemes converge to the reference solution well, which can be seen in Figure 2 for the cuts of $p = u + v$ at the final time $t = 2000$. In Figure 2(b), we can see that the higher order schemes produce results closer to the reference solution. Converged solutions in Figure 3(d) show that u and v almost overlap with each other, and numerical solutions u and v generated by the WENO-3 scheme and the WENO-5 scheme also overlap with each other, while u and v generated by the upwind scheme still show a slight translation.

Example 4. In this example, we consider the traveling pulses problem. We choose the parameters as

$$\begin{aligned} \gamma &= 0.1, & a_1 &= 0.2, & a_2 &= 0.9, \\ q_a &= 1.6, & q_{al} &= 2, & q_r &= 0.5. \end{aligned}$$

The initial condition is the same as in Example 3.

Here, we use 200 grid points for the WENO-3 scheme, the WENO-5 scheme and the first order upwind scheme. Also, the numerical solution using the upwind scheme with 6000 grid point is taken as the converged reference solution. In Figure 4, we plot the total density $p = u + v$ from time $t = 1500$ to $t = 2000$. The numerical

24 *Y. Jiang, C.-W. Shu, and M. Zhang*

solutions are traveling for all schemes. In Figure 5, we give a cut of $p = u + v$ at the final time $t = 2000$, and we can see that the higher order schemes produce results closer to the converged reference solution.

Example 5. In this example, we test the system (1.1) with discontinuous initial conditions

$$u(x, 0) = \begin{cases} 1, & 0 \leq x \leq 4 \\ 0, & 4 < x < 10. \end{cases} \quad (5.8)$$

$$v(x, 0) = \begin{cases} 0, & 0 < x < 6 \\ 1, & 6 \leq x \leq 10. \end{cases} \quad (5.9)$$

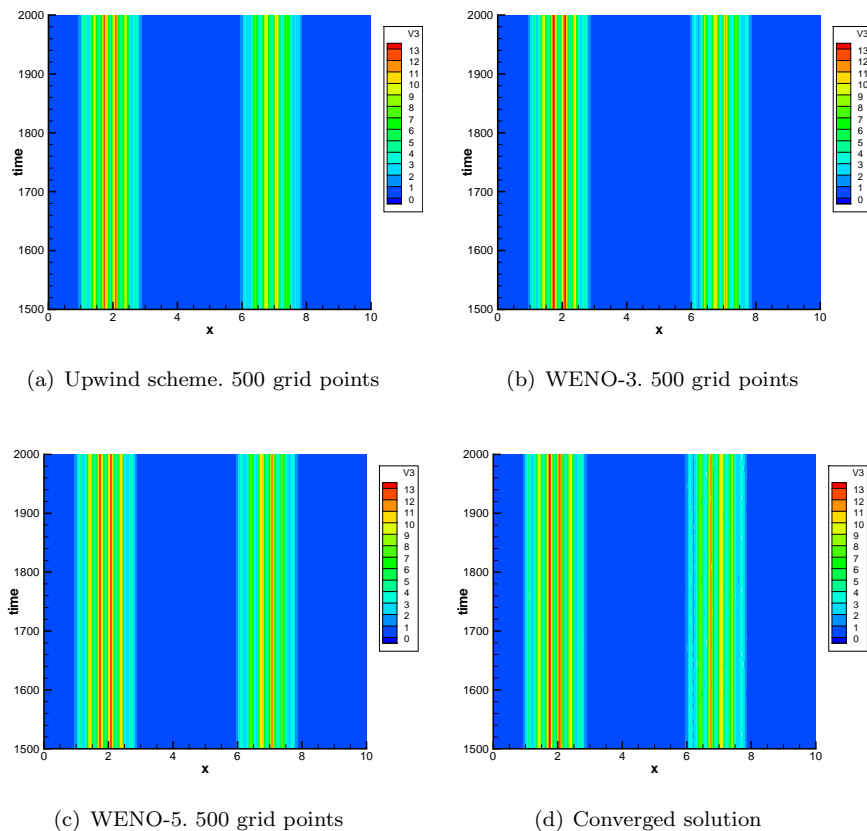


Fig. 1. Example 3: Stationary pulses. $u + v$ from $t = 1500$ to $t = 2000$.

We choose the parameters as

$$\begin{aligned} \gamma &= 0.1, & a_1 &= 0.2, & a_2 &= 0.9, \\ q_a &= 1.6, & q_{al} &= 2.0, & q_r &= 0.5. \end{aligned}$$

In Figure 6, we plot the numerical solutions u at time $t = 2$, with the first order upwind scheme, the WENO-3 scheme with and without the PP-limiter, and the WENO-5 scheme with and without the PP-limiter. We also test the third order finite difference (FD-3) scheme without the PP-limiter, which is the third order finite difference WENO scheme using the linear weights. Numerical solution obtained with the first order upwind scheme using 2000 grid points are used as a converged reference solution. Minimum values of the u -component at $t = 2$ of the WENO-3 scheme and the WENO-5 scheme are shown in Table 10. We can see that without the nonlinear weights, the FD-3 scheme has oscillations near the interfaces. Comparing Figure 6(c), Figure 6(d), Figure 6(e) and Figure 6(f), we can see that the PP-limiter does not affect the non-oscillatory discontinuity transitions of WENO schemes when maintaining positivity.

Table 10. Example 5: Minimum values of the u -component at $t = 2$.

	with the PP-limiter	without the PP-limiter
WENO-3	1.000E-16	-5.055E-08
WENO-5	1.000E-16	-1.346E-07

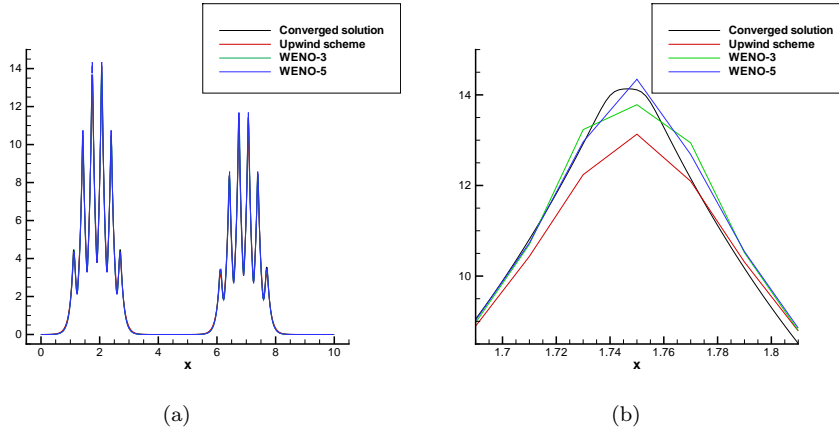


Fig. 2. Example 3: Stationary pulses. Cut of $p = u + v$ at time $T = 2000$. Figure 2(b) is the enlarged view of Figure 2(a)

6. Conclusion

In this paper, we discuss high order finite difference WENO schemes coupled with total variation diminishing (TVD) Runge-Kutta (RK) temporal integration for a non-local hyperbolic system of a correlated random walk model. A positivity-preserving limiter is introduced to guarantee positivity of the solution. Analysis is given to show that when the limiter is applied to a third order finite difference scheme with third order TVD-RK time discretization solving this model, the scheme can maintain third order accuracy for both the source and the numerical fluxes, under the standard CFL condition. Numerical results are provided to demonstrate these methods up to fifth order accuracy.

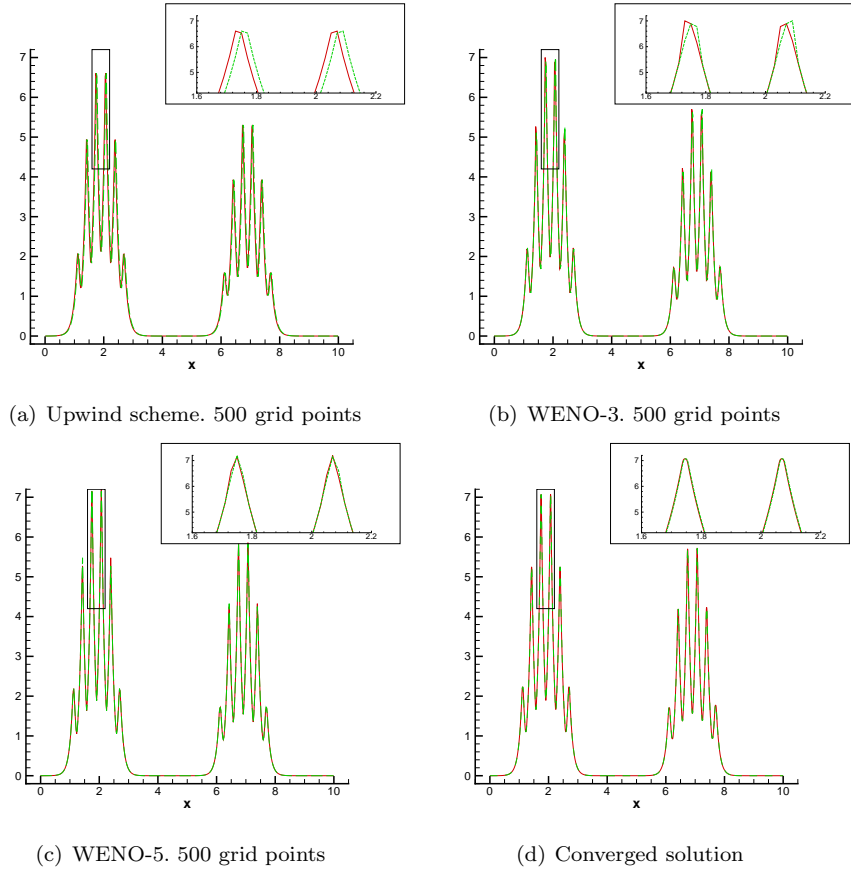


Fig. 3. Example 3: Stationary pulses. u and v at the final time $t = 2000$. The solid lines are the u -component and the dash lines are the v -component. The small figures are the enlarged view inside the rectangles.

Appendix A. Proof of some lemmas

We will give the proof of some of the technical lemmas in this section as an appendix.

A.1. The proof of Lemma 4.1

Suppose $u^n(x), v^n(x)$ is the solution at time t^n . With the third order TVD Runge-Kutta

$$\begin{aligned} u^{(1)} &= u^n + \Delta t L(u^n) \\ u^{(2)} &= \frac{3}{4}u^n + \frac{1}{4}u^{(1)} + \frac{1}{4}\Delta t L(u^{(1)}) \\ u^{n+1} &= \frac{1}{3}u^n + \frac{2}{3}u^{(2)} + \frac{2}{3}\Delta t L(u^{(2)}) \end{aligned} \tag{A.1}$$

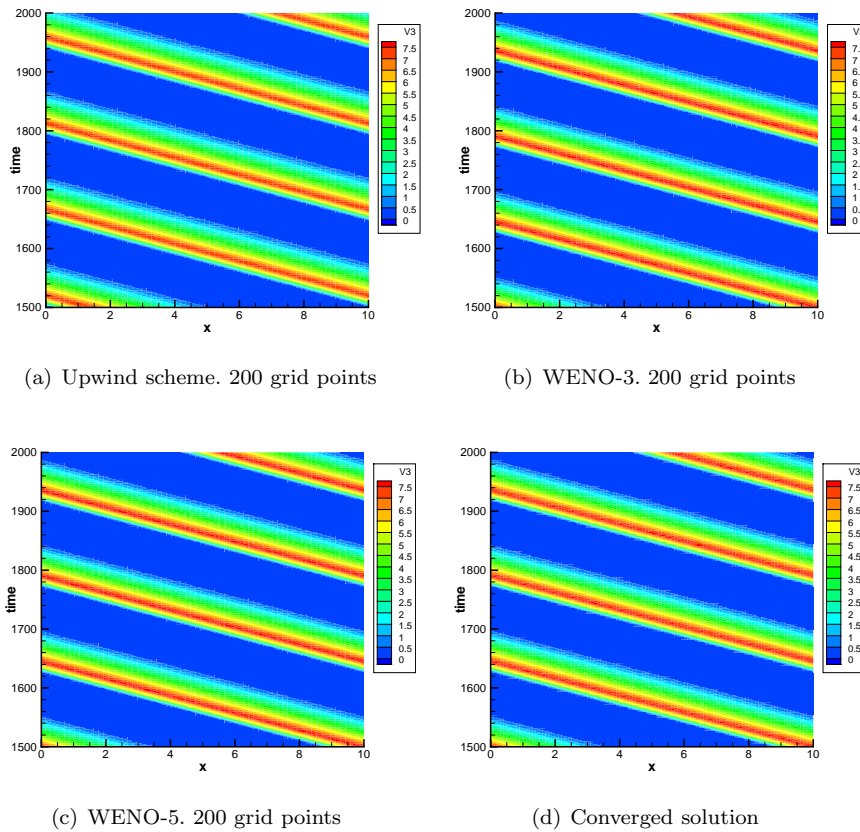


Fig. 4. Example 4: Traveling pulses. $u + v$ from $t = 1500$ to $t = 2000$.

28 *Y. Jiang, C.-W. Shu, and M. Zhang*

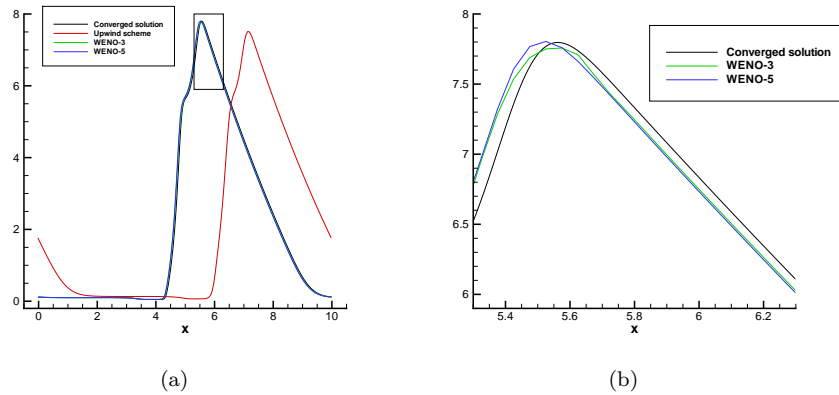


Fig. 5. Example 4: Traveling pulses. Cut of $p = u + v$ at time $T = 2000$. Fig.5(b) is the enlarged view inside the rectangle in fig.5(a)

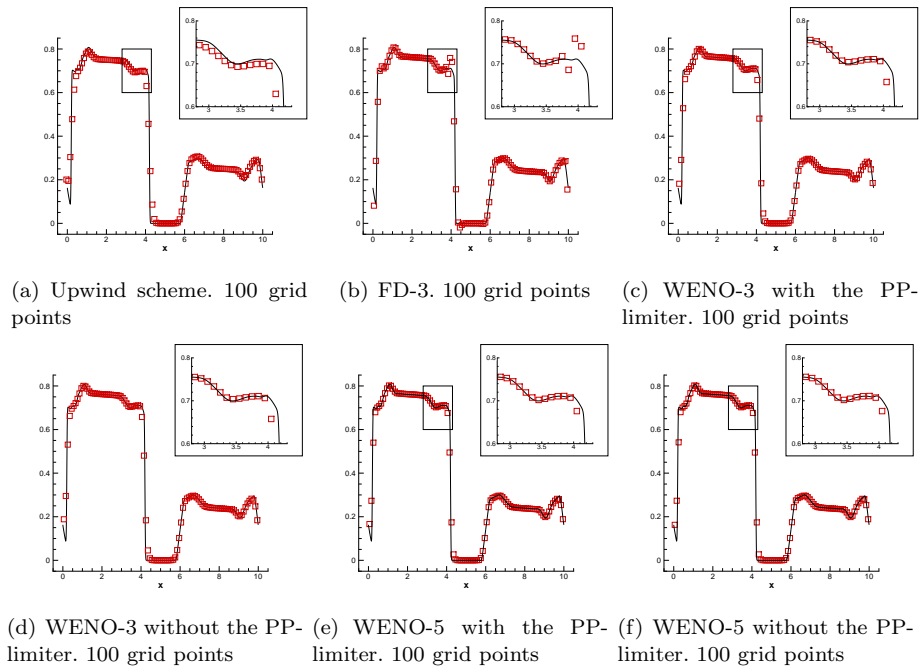


Fig. 6. Example 5: The u -component at $t = 2$. The solid lines are converged solutions and the symbols are numerical solutions. The small figures are the enlarged view inside the rectangles.

we define the functions $\tilde{u}^{(1)}$ and $\tilde{u}^{(2)}$ as

$$\begin{aligned}\tilde{u}^{(1)}(x) &= u^n(x) + \Delta t(-\gamma u_x^n + g[u^n, v^n, x]) \\ \tilde{u}^{(2)}(x) &= \frac{3}{4}u^n(x) + \frac{1}{4}\tilde{u}^{(1)}(x) + \frac{1}{4}\Delta t(-\gamma \tilde{u}_x^{(1)} + g[\tilde{u}^{(1)}, \tilde{v}^{(1)}, x])\end{aligned}\quad (\text{A.2})$$

Since

$$\begin{aligned}u_j^{(1)} &= u_j^n + \Delta t\left(-\frac{\hat{H}_{j+1/2}^n - \hat{H}_{j-1/2}^n}{\Delta x} + g[u^n, v^n, x_j]\right) \\ u_j^{(2)} &= \frac{3}{4}u_j^n + \frac{1}{4}u_j^{(1)} + \frac{1}{4}\Delta t\left(-\frac{\hat{H}_{j+1/2}^{(1)} - \hat{H}_{j-1/2}^{(1)}}{\Delta x} + g[u^{(1)}, u^{(1)}, x_j]\right)\end{aligned}\quad (\text{A.3})$$

where $\hat{H}_{j+1/2}^n$ and $\hat{H}_{j+1/2}^{(1)}$ are the numerical fluxes with third order accuracy w.r.t. u^n and $u^{(1)}$. Hence we can get

$$u_j^{(1)} = \tilde{u}^{(1)}(x_j) + O(\Delta t \Delta x^3)$$

$$u_j^{(2)} = \tilde{u}^{(2)}(x_j) + O(\Delta t \Delta x^3)$$

We also have similar definitions and results for the v -component.

In the proof below, all unmarked quantities are evaluated at time level n . Since

$$\begin{aligned}\tilde{u}^{(1)} &= u^n + \Delta t(-\gamma u_x + g[u, v, x]) \\ \tilde{v}^{(1)} &= v^n + \Delta t(\gamma v_x - g[u, v, x])\end{aligned}$$

we have

$$\begin{aligned}y_1[\tilde{u}^{(1)}, \tilde{v}^{(1)}, x] &= y_1[u + \Delta t(-\gamma u_x + g), v + \Delta t(\gamma v_x - g), x] \\ &= y_1[u, v, x] + \Delta t y_1[-\gamma u_x + g, \gamma v_x - g, x] \\ y_2[\tilde{u}^{(1)}, \tilde{v}^{(1)}, x] &= y_2[u + \Delta t(-\gamma u_x + g), v + \Delta t(\gamma v_x - g), x] \\ &= y_2[u, v, x] + \Delta t y_2[-\gamma u_x + g, \gamma v_x - g, x]\end{aligned}$$

and

$$\begin{aligned}\lambda_1[\tilde{u}^{(1)}, \tilde{v}^{(1)}, x] &= a_1 + a_2 f(y_1[\tilde{u}^{(1)}, \tilde{v}^{(1)}, x]) \\ &= a_1 + a_2 f(y_1[u, v, x]) + a_2 \Delta t f'(y_1[u, v, x]) y_1[-\gamma u_x + g, \gamma v_x - g, x] + O(\Delta t^2) \\ &= \lambda_1 + a_2 \Delta t f'(y_1[u, v, x]) y_1[-\gamma u_x + g, \gamma v_x - g, x] + O(\Delta t^2) \\ \lambda_2[\tilde{u}^{(1)}, \tilde{v}^{(1)}, x] &= a_1 + a_2 f(y_2[\tilde{u}^{(1)}, \tilde{v}^{(1)}, x]) \\ &= a_1 + a_2 f(y_2[u, v, x]) + a_2 \Delta t f'(y_2[u, v, x]) y_2[-\gamma u_x + g, \gamma v_x - g, x] + O(\Delta t^2) \\ &= \lambda_2 + a_2 \Delta t f'(y_2[u, v, x]) y_2[-\gamma u_x + g, \gamma v_x - g, x] + O(\Delta t^2)\end{aligned}$$

30 *Y. Jiang, C.-W. Shu, and M. Zhang*

Hence, we can get

$$g[\tilde{u}^{(1)}, \tilde{v}^{(1)}, x] = -\lambda_1[\tilde{u}^{(1)}, \tilde{v}^{(1)}, x]\tilde{u}^{(1)} + \lambda_2[\tilde{u}^{(1)}, \tilde{v}^{(1)}, x]\tilde{v}^{(1)} \quad (\text{A.4})$$

$$\begin{aligned} &= -\lambda_1 u + \lambda_2 v + \Delta t \{-a_2 f'(y_1[u, v, x])y_1[-\gamma u_x + g, \gamma v_x - g, x]u \\ &\quad - \lambda_1(-\gamma u_x + g) + a_2 f'(y_2[u, v, x])y_2[-\gamma u_x + g, \gamma v_x - g, x]v \\ &\quad + \lambda_2(\gamma v_x - g)\} + O(\Delta t^2) \end{aligned} \quad (\text{A.5})$$

With the definitions, we obtain $\tilde{u}^{(2)}$ and $\tilde{v}^{(2)}$:

$$\begin{aligned} \tilde{u}^{(2)} &= \frac{3}{4}u_j + \frac{1}{4}\tilde{u}_j^{(1)} + \frac{1}{4}\Delta t(-\gamma\tilde{u}_x^{(1)} + g[\tilde{u}^{(1)}, \tilde{v}^{(1)}, x]) \\ &= u^n + \frac{1}{2}\Delta t(-\gamma u_x + g) \\ &\quad + \frac{1}{4}\Delta t^2\{\gamma^2 u_{xx} - \gamma(-\lambda_{1,x}u - \lambda_1 u_x + \lambda_{2,x}v + \lambda_2 v_x) \\ &\quad - a_2 f'(y_1[u, v, x])y_1[-\gamma u_x + g, \gamma v_x - g, x]u - \lambda_1(-\gamma u_x + g) \\ &\quad + a_2 f'(y_2[u, v, x])y_2[-\gamma u_x + g, \gamma v_x - g, x]v + \lambda_2(\gamma v_x - g)\} \\ &\quad + O(\Delta t^3) \\ \tilde{v}^{(2)} &= \frac{3}{4}v_j + \frac{1}{4}\tilde{v}_j^{(1)} + \frac{1}{4}\Delta t(\gamma\tilde{v}_x^{(1)} - g[\tilde{u}^{(1)}, \tilde{v}^{(1)}, x]) \\ &= v + \frac{1}{2}\Delta t(\gamma v_x - g) \\ &\quad + \frac{1}{4}\Delta t^2\{\gamma^2 v_{xx} - \gamma(-\lambda_{1,x}u - \lambda_1 u_x + \lambda_{2,x}v + \lambda_2 v_x) \\ &\quad + a_2 f'(y_1[u, v, x])y_1[-\gamma u_x + g, \gamma v_x - g, x]u + \lambda_1(-\gamma u_x + g) \\ &\quad - a_2 f'(y_2[u, v, x])y_2[-\gamma u_x + g, \gamma v_x - g, x]v - \lambda_2(\gamma v_x - g)\} \\ &\quad + O(\Delta t^3) \end{aligned}$$

And we repeat the procedure of $g[\tilde{u}^{(1)}, \tilde{v}^{(1)}, x]$ to get $g[\tilde{u}^{(2)}, \tilde{v}^{(2)}, x]$, therefore

$$\begin{aligned} g[\tilde{u}^{(2)}, \tilde{v}^{(2)}, x] &= -\lambda_1 u + \lambda_2 v + \frac{1}{2}\Delta t\{-a_2 f'(y_1[u, v, x]) \cdot y_1[-\gamma u_x + g, \gamma v_x - g, x]u \\ &\quad - \lambda_1(-\gamma u_x + g) + a_2 f'(y_2[u, v, x]) \cdot y_2[-\gamma u_x + g, \gamma v_x - g, x]v \\ &\quad + \lambda_2(\gamma v_x - g)\} + O(\Delta t^2) \end{aligned} \quad (\text{A.6})$$

Since

$$y_1[-\gamma u_x + g, \gamma v_x - g, x] = y_1[u_t, v_t, x] = y_{1,t}[u, v, x]$$

$$y_2[-\gamma u_x + g, \gamma v_x - g, x] = y_2[u_t, v_t, x] = y_{2,t}[u, v, x]$$

we write the above expressions as

$$g[\tilde{u}^{(1)}, \tilde{v}^{(1)}, x] = g + \Delta t(-\lambda_{1,t}u - \lambda_1 u_t + \lambda_{2,t}v + \lambda_2 v_t) + O(\Delta t^2) \quad (\text{A.7})$$

$$g[\tilde{u}^{(2)}, \tilde{v}^{(2)}, x] = g + \frac{1}{2}\Delta t(-\lambda_{1,t}u - \lambda_1 u_t + \lambda_{2,t}v + \lambda_2 v_t) + O(\Delta t^2) \quad (\text{A.8})$$

$$\begin{aligned} \tilde{u}^{(2)} &= u + \frac{1}{2}\Delta t(-\gamma u_x + g) + \frac{1}{4}\Delta t^2\{\gamma^2 u_{xx} - \gamma(-\lambda_{1,x}u - \lambda_1 u_x + \lambda_{2,x}v + \lambda_2 v_x) \\ &\quad + (-\lambda_{1,t}u - \lambda_1 u_t + \lambda_{2,t}v + \lambda_2 v_t)\} + O(\Delta t^3) \end{aligned} \quad (\text{A.9})$$

$$\begin{aligned} \tilde{v}^{(2)} &= v + \frac{1}{2}\Delta t(\gamma u_x - g) + \frac{1}{4}\Delta t^2\{\gamma^2 v_{xx} - \gamma(-\lambda_{1,x}u - \lambda_1 u_x + \lambda_{2,x}v + \lambda_2 v_x) \\ &\quad - (-\lambda_{1,t}u - \lambda_1 u_t + \lambda_{2,t}v + \lambda_2 v_t)\} + O(\Delta t^3) \end{aligned} \quad (\text{A.10})$$

Hence

$$\begin{aligned} \hat{G}_j^{rk} &= \frac{1}{6}g[u^n, v^n, x_j] + \frac{1}{6}g[\tilde{u}^{(1)}, \tilde{v}^{(1)}, x_j] + \frac{2}{3}g[\tilde{u}^{(2)}, \tilde{v}^{(2)}, x_j] + O(\Delta x^3) \\ &= g_j + \frac{1}{2}\Delta t(-\lambda_{1,t}u - \lambda_1 u_t + \lambda_{2,t}v + \lambda_2 v_t) + O(\Delta t^2 + \Delta x^3) \end{aligned} \quad (\text{A.11})$$

If we use a third order finite difference scheme for the spatial discretization, we have

$$\hat{H}_{j+1/2} = \frac{13}{12}f_{j+1/2} - \frac{1}{24}f_{j-1/2} - \frac{1}{24}f_{j+3/2} + O(\Delta x^3)$$

So if we expand $H_{j+1/2}^{rk}$ at x_j for the u -component with $f(u) = \gamma u$, we can get

$$\begin{aligned} \hat{H}_{j+1/2}^{rk} &= \frac{1}{6}\left(\frac{13}{12}f(u^n)_{j+1/2} - \frac{1}{24}f(u^n)_{j-1/2} - \frac{1}{24}f(u^n)_{j+3/2}\right) \\ &\quad + \frac{1}{6}\left(\frac{13}{12}f(\tilde{u}^{(1)})_{j+1/2} - \frac{1}{24}f(\tilde{u}^{(1)})_{j-1/2} - \frac{1}{24}f(\tilde{u}^{(1)})_{j+3/2}\right) \\ &\quad + \frac{2}{3}\left(\frac{13}{12}f(\tilde{u}^{(2)})_{j+1/2} - \frac{1}{24}f(\tilde{u}^{(2)})_{j-1/2} - \frac{1}{24}f(\tilde{u}^{(2)})_{j+3/2}\right) \\ &\quad + O(\Delta x^3) \\ &= \gamma u_j + \Delta x\left(\frac{1}{2}(1 - \lambda\gamma)\gamma u_x + \frac{1}{2}\lambda\gamma g\right) + \Delta x^2\left\{\frac{1}{2}\left(\frac{1}{3}\gamma^2\lambda^2 - \frac{1}{2}\lambda\gamma + \frac{1}{6}\right)u_{xx} \right. \\ &\quad + \frac{1}{2}\left(\frac{1}{3}\lambda\gamma + \frac{1}{2}\right)(-\lambda_{1,x}u - \lambda_1 u_x + \lambda_{2,x}v + \lambda_2 v_x) \\ &\quad + \frac{1}{6}\lambda^2\gamma(-\lambda_{1,t}u - \lambda_1 u_t + \lambda_{2,t}v + \lambda_2 v_t)\} \\ &\quad + O(\Delta x^3 + \Delta t^3) \end{aligned} \quad (\text{A.12})$$

A.2. The proof of Lemma 4.2

We will find the u -component values along the characteristic line

$$l : x|_l = \gamma(t - t^*) + x^*$$

32 *Y. Jiang, C.-W. Shu, and M. Zhang*

We denote $w_l(t; x^*, t^*)$ as $w_l(t)$, $l = 1, 2$. Then we can get

$$\begin{aligned}\frac{dw_1}{dt} &= \gamma u_x + u_t = g \\ \frac{dw_2}{dt} &= \gamma v_x + v_t = 2\gamma v_x - g\end{aligned}$$

Hence,

$$w_1(t) = w_1(t^*) + \int_{t^*}^t g[u(x, \tau), v(x, \tau), \gamma(\tau - t^*) + x^*] d\tau$$

Because

$$\begin{aligned}w_1(\tau) &= w_1(t^*) + (\tau - t^*) \frac{dw_1}{dt}(t^*) + O((\tau - t^*)^2) \\ &= w_1(t^*) + (\tau - t^*) (u_t + \gamma u_x)|_{(x^*, t^*)} + O((\tau - t^*)^2) \\ w_2(\tau) &= w_2(t^*) + (\tau - t^*) \frac{dw_2}{dt}(t^*) + O((\tau - t^*)^2) \\ &= w_2(t^*) + (\tau - t^*) (v_t + \gamma v_x)|_{(x^*, t^*)} + O((\tau - t^*)^2)\end{aligned}$$

$$\begin{aligned}p(\gamma(\tau - t^*) + x^*, \tau) &= w_1(\tau) + w_2(\tau) \\ &= w_1(t^*) + w_2(t^*) + (\tau - t^*) (u_t + v_t + \gamma(u_x + v_x))|_{(x^*, t^*)} + O((\tau - t^*)^2) \\ &= p(x^*, t^*) + (\tau - t^*) (p_t(x^*, t^*) + \gamma p_x(x^*, t^*)) + O((\tau - t^*)^2)\end{aligned}$$

we can get

$$\begin{aligned}& q_r \int_0^\infty K_r(s) \cdot [p(\gamma(\tau - t^*) + x^* + s, \tau) - p(\gamma(\tau - t^*) + x^* - s, \tau)] ds \\ &= q_r \int_0^\infty K_r(s) \cdot [p(x^* + s, t^*) + (\tau - t^*) (p_t(x^* + s, t^*) + \gamma p_x(x^* + s, t^*)) + O((\tau - t^*)^2) \\ &\quad - p(x^* - s, t^*) - (\tau - t^*) (p_t(x^* - s, t^*) + \gamma p_x(x^* - s, t^*)) + O((\tau - t^*)^2)] ds \\ &= q_r \int_0^\infty K_r(s) \cdot [p(x^* + s, t^*) - p(x^* - s, t^*)] ds \\ &\quad + (\tau - t^*) q_r \int_0^\infty K_r(s) \cdot [p_t(x^* + s, t^*) - p_t(x^* - s, t^*)] ds \\ &\quad + \gamma(\tau - t^*) q_r \int_0^\infty K_r(s) \cdot [p_x(x^* + s, t^*) - p_x(x^* - s, t^*)] ds \\ &\quad + O((\tau - t^*)^2)\end{aligned}$$

Thus

$$\begin{aligned}& y_1[u(x, \tau), v(x, \tau), \gamma(\tau - t^*) + x^*] \\ &= q_r \int_0^\infty K_r(s) [p(\gamma(\tau - t^*) + x^* + s, \tau) - p(\gamma(\tau - t^*) + x^* - s, \tau)] ds \\ &\quad - q_a \int_0^\infty K_a(s) [p(\gamma(\tau - t^*) + x^* + s, \tau) - p(\gamma(\tau - t^*) + x^* - s, \tau)] ds\end{aligned}$$

$$\begin{aligned}
 & + q_{al} \int_0^\infty K_{al}(s)[v(\gamma(\tau - t^*) + x^* + s, \tau) - u(\gamma(\tau - t^*) + x^* - s, \tau)]ds \\
 = & y_1[u(x, t^*), v(x, t^*), x^*] + (\tau - t^*) \cdot y_1[u_t(x, t^*), v_t(x, t^*), x^*] \\
 & + \gamma(\tau - t^*) \cdot y_1[u_x(x, t^*), v_x(x, t^*), x^*] + O((\tau - t^*)^2) \\
 = & y_1[u(x, t^*), v(x, t^*), x^*] + (\tau - t^*) \cdot y_{1,t}[u(x, t^*), v(x, t^*), x^*] \\
 & + \gamma(\tau - t^*) \cdot y_{1,x}[u(x, t^*), v(x, t^*), x^*] + O((\tau - t^*)^2)
 \end{aligned}$$

and

$$\begin{aligned}
 & \lambda_1[u(x, \tau), v(x, \tau), \gamma(\tau - t^*) + x^*] \\
 = & a_1 + a_2 f(y_1[u(x, \tau), v(x, \tau), \gamma(\tau - t^*) + x^*]) \\
 = & a_1 + a_2 f(y_1[u(x, t^*), v(x, t^*), x^*] \\
 & + a_2(\tau - t^*) f'(y_1[u(x, t^*), v(x, t^*), x^*]) \cdot y_{1,t}[u(x, t^*), v(x, t^*), x^*] \\
 & + a_2 \gamma(\tau - t^*) f'(y_1[u(x, t^*), v(x, t^*), x^*]) \cdot y_{1,x}[u(x, t^*), v(x, t^*), x^*] \\
 & + O((\tau - t^*)^2) \\
 = & \lambda_1[u(x, t^*), v(x, t^*), x^*] + (\tau - t^*) \lambda_{1,t}[u(x, t^*), v(x, t^*), x^*] + \gamma(\tau - t^*) \lambda_{1,x}[u(x, t^*), v(x, t^*), x^*] \\
 & + O((\tau - t^*)^2)
 \end{aligned}$$

Similarly,

$$\begin{aligned}
 & \lambda_2[u(x, \tau), v(x, \tau), \gamma(\tau - t^*) + x^*] \\
 = & \lambda_2[u(x, t^*), v(x, t^*), x^*] + (\tau - t^*) \lambda_{2,t}[u(x, t^*), v(x, t^*), x^*] + \gamma(\tau - t^*) \lambda_{2,x}[u(x, t^*), v(x, t^*), x^*] \\
 & + O((\tau - t^*)^2)
 \end{aligned}$$

Hence

$$\begin{aligned}
 & g[u(x, \tau), v(x, \tau), \gamma(\tau - t^*) + x^*] \\
 = & -\lambda_1[u(x, t^*), v(x, t^*), \gamma(\tau - t^*) + x^*] \cdot w_1(\tau) + \lambda_2[u(x, t^*), v(x, t^*), \gamma(\tau - t^*) + x^*] \cdot w_2(\tau) \\
 = & -\lambda_1[u(x, t^*), v(x, t^*), x^*] \cdot w_1(t^*) + \lambda_2[u(x, t^*), v(x, t^*), x^*] \cdot w_2(t^*) \\
 & + (\tau - t^*) \cdot [-\lambda_{1,t}u - \lambda_1 u_t + \lambda_{2,t}v + \lambda_2 v_t + \gamma(-\lambda_{1,x}u - \lambda_1 u_x + \lambda_{2,x}v + \lambda_2 v_x)]|_{(x^*, t^*)} \\
 & + O((\tau - t^*)^2)
 \end{aligned}$$

and

$$\begin{aligned}
 & \int_{t^*}^t g[u(x, \tau), v(x, \tau), \gamma(\tau - t^*) + x^*] dt \\
 = & (t - t^*) \cdot g[u(x, t^*), v(x, t^*), x^*] + \frac{1}{2}(t - t^*)^2 \cdot \{-\lambda_{1,t}u - \lambda_1 u_t + \lambda_{2,t}v + \lambda_2 v_t \\
 & + \gamma(-\lambda_{1,x}u - \lambda_1 u_x + \lambda_{2,x}v + \lambda_2 v_x)\}|_{(x^*, t^*)} + O((\tau - t^*)^3)
 \end{aligned}$$

Thus

$$u(\gamma(t - t^*) + x^*, t^*)$$

34 *Y. Jiang, C.-W. Shu, and M. Zhang*

$$\begin{aligned}
 &= u(x^*, t^*) + (t - t^*) \cdot g[u(x, t^*), v(x, t^*), x^*] \\
 &\quad + \frac{1}{2}(t - t^*) \cdot \{-\lambda_{1,t}u - \lambda_1 u_t + \lambda_{2,t}v + \lambda_2 v_t + \gamma(-\lambda_{1,x}u - \lambda_1 u_x + \lambda_{2,x}v + \lambda_2 v_x)\}|_{(x^*, t^*)} \\
 &\quad + O((t - t^*)^3)
 \end{aligned}$$

Acknowledgment

Research of Y. Jiang was supported by the USTC Special Grant for Postgraduate Research, Innovation and Practice and by the CAS Special Grant for Postgraduate Research, Innovation and Practice. Research of C.-W. Shu was supported by AFOSR grant F49550-12-1-0399 and NSF grant DMS-1112700. Research of M. Zhang was supported by NSFC grants 11071234, 91130016 and 91024025.

References

1. D. Balsara and C.-W. Shu, Monotonicity preserving weighted essentially non-oscillatory schemes with increasingly high order of accuracy, *J. Comput. Phys.* **160** (2000) 405–452.
2. R. Eftimie, G. de Vries and M.A. Lewis, Complex spatial group patterns result from different animal communication mechanisms, *P. Natl. Acad. Sci.* **104** (2007) 6974–6979.
3. R. Eftimie, G. de Vries, M.A. Lewis and F. Lutscher, Modeling group formation and activity patterns in self-organizing collectives of individual, *B. Math. Biol.* **69** (2007) 1537–1565.
4. S. Goldstein, On diffusion by the discontinuous movements and the telegraph equation, *Q. J. Mech. Appl. Math.* **4** (1951) 129–156.
5. H. Hasimoto, Exact solution of a certain semi-linear system of partial differential equations related to a migrating predation problem, *P. Jpn. Acad. A-Math.* **50** (1974) 623–627.
6. G. Jiang and C.-W. Shu, Efficient implementation of weighted ENO schemes, *J. Comput. Phys.* **126** (1996) 202–228.
7. M. Kac, A stochastic model related to the telegraphers equation, *Rocky Mt. J. Math.*, **4** (1974) 497–509.
8. C. Liang and Z. Xu, Parametrized maximum-principle-preserving flux limiters for high order schemes solving multi-dimensional scalar hyperbolic conservation laws, *J. Sci. Comput.* **58** (2014) 41–60.
9. X.D. Liu, S. Osher and T. Chan, Weighted essentially non-oscillatory schemes, *J. Comput. Phys.* **115** (1994) 200–212.
10. J. Lu, C.-W. Shu and M. Zhang, Stability analysis and a priori error estimate of explicit Runge-Kutta discontinuous Galerkin methods for correlated random walk with density-dependent turning rates, *Sci. China Math.* **56** (2013) 2645–2676.
11. F. Lutscher, Modeling alignment and movement of animals and cells, *J. Math. Biol.* **45** (2002) 234–260.
12. F. Lutscher and A. Stevens, Hyperbolic models for chemotaxis in 1-D, *Nonlinear Anal.-Real.* **1** (2000) 409–433.
13. F. Lutscher and A. Stevens, Emerging patterns in a hyperbolic model for locally interacting cell systems, *J. Nonlinear Sci.* **12** (2002) 619–640.
14. C.-W. Shu, High order weighted essentially non-oscillatory schemes for convection dominated problems, *SIAM Rev.* **51** (2009) 82–126.

15. C.-W. Shu and S. Osher, Efficient implementation of essentially non-oscillatory shock-capturing schemes, *J. Comput. Phys.* **77** (1988) 439–471.
16. T. Xiong, J.-M. Qiu and Z. Xu, A parametrized maximum principle preserving flux limiter for finite difference RK-WENO schemes with applications in incompressible flows, *J. Comput. Phys.* **252** (2013) 310–331.
17. T. Xiong, J.-M. Qiu and Z. Xu, Parameterized positive preserving flux limiters for the high order finiter difference WENO scheme solving compressible Euler equation, *J. Comput. Phys.* submitted.
18. Z. Xu, Parametrized maximum principle preserving flux limiters for high order scheme solving hyperbolic conservation laws: one-dimensional scalar problem, *Math. Comput.* **83** (2014) 2213–2238.
19. X. Zhang and C.-W. Shu, On maximum-principle-satisfying high order schemes for scalar conservation laws, *J. Comput. Phys.* **229** (2010) 3091–3120.
20. X. Zhang and C.-W. Shu, On positivity preserving high order discontinuous Galerkin schemes for compressible Euler equations on rectangular meshes, *J. Comput. Phys.* **229** (2010) 8918–8934.
21. X. Zhang and C.-W. Shu, Maximum-principle-satisfying and positivity-preserving high order schemes for conservation laws: Survey and new developments, *P. Roy. Soc. A* **467** (2011) 2752–2776.
22. X. Zhang and C.-W. Shu, Positivity-preserving high order finite difference WENO schemes for compressible Euler equations, *J. Comput. Phys.* **231** (2012) 2245–2258.
23. X. Zhang, Y. Xia and C.-W. Shu, Maximum-principle-satisfying and positivity-preserving high order discontinuous Galerkin schemes for conservation laws on triangular meshes, *J. Sci. Comput.* **50** (2012) 29–62.